Republic of Iraq
Ministry of Higher Education
&Scientific Research
AL-Muthanna University
College of Science
Department of Chemistry

Hydrolysis of cellulose and glucose onto silica-pyridine sulfonic acid

A thesis submitted to the Council of College of Science /
Al-Muthanna University as partial Fulfillment of the
Requirement for the Degree of
Master of Science in Chemistry

By
Hussein Abdel Bari Zuweid
B. Sc. In Chemistry 2009

Supervised By
Prof. Dr. Kasim Mohammed Hello

2023 A.D 1444 A.H

صدق الله العظيم

سورة المجادلة – الاية ١١

Certification of the Supervisor

I certify that this thesis entitled **"Hydrolysis of cellulose and glucose onto silica-pyridine sulfonic acid"** was done under my guidance in the Chemistry Department of Al-Muthanna University College of Science as part of the requirements for the Master of Science in Chemistry.

Signature:

Supervisor: Prof. Dr. Kasim Mohammed Hello

Department of Chemistry/. College of Science/Al-Muthanna University

Data: / / 2023

In view of the available recommendations, I forward this thesis for debate

By the examining committee

Signature:

Assist. Prof. Dr. Azal Shakir Waheeb

Head Department of Chemistry/. College of Science /Al-Muthanna University

Data: / / 2023

Dedication

To those who sacrificed themselves for the sake of the homeland and the sanctities of

the souls of the martyrs of the popular populist crowd and the heroic security forces

To my dear parents, who are the reason behind my

Existence and success

Acknowledgement

Initially, I want to thank the almighty Allah for giving me the strength and guidance throughout my entire life and during this work in particular. I wish also to express my deepest gratitude to my supervisor **Prof. Dr. Kasim Mohammed Hello** for his continuous support, invaluable suggestions and great contributions since the very beginning of this work.

Also, I want to thank all faculty members of Department of Chemistry in the College of Science at the University of Al-Muthanna, for their precious support. Finally, I want to thank my family and my friends for their continual support throughout this journey. They were my source of encouragement along the way.

Hussein

List of contents

List of Tables

	List of Symbols and Abbreviations
Abbreviation	**Term**
5-HMF	hydroxylmethylfurfural
BET	Brunauer-Emmett-Teller
CHNS	Carbon, hydrogen, nitrogen and sulfur elemental analysis
CPTES	3-(Chloropropyl) triethoxysilane
DMA	N, N-dimethylaceamide
DMF	Dimethylformamide
DMI	1,3-dimethyl-2-imidazolidinone
DNS	Dinitrosalycilic acid
FT-IR	Fourier Transform Infrared
H3	Hysteresis loop type 3
IUPAC	International union of pure and applied chemistry
P/Po	P/Po Relative pressure
RH	Rice Husk
RHA	Rice Husk Ash
RHACCl	RHA immobilized with 3-chloroprpyltriethoxysilane.
RHAPSA@Dir	Preparation of heterogeneous catalyst (direct method)
RHAPSA@Ref	Preparation of heterogeneous catalyst (reflux method)
SEM	Scanning Electron Microscopy
Si-OH	Silanol group
Si-O-Si	Siloxane group
Sol	Colloidal suspension

T	Temperature
TEM	Transmission Electron Microscopy
TGA	Thermal Gravimetric Analysis
XRD	X-Ray diffraction

Abstract

In this study, silica was extracted from rice husk by washing rice husk many times with distilled water, and then treated with 1.0 M of Nitric acid; finally, it was burned in an oven at 800 ^{o}C. Using method Sol-gel the resulting silica was converted into sodium silicate after dissolving it with a solution (1.0M) of sodium hydroxide, then it was reacted with CPTES to produce a silica with the functional group CH_2-Cl and the symbol RHACCl.

Loading pyridine sulfonic acid on the surface of silica in two ways: the direct method, where pyridine sulfonic acid, CPTES, and sodium silicate were added to the aqueous solution, then the mixture was titrated against HNO_3 (3.0N), and the reflux method, where RHACCl and pyridine sulfonic acid were added to the toluene solvent and at a temperature of 120°C for 48 hours to form a heterogeneous catalyst symbol, RHAPSA@Dir and RHAPSA@Ref, respectively.

The prepared catalyst was identified by several techniques, including elemental analysis (CHNS), where the percentages of nitrogen and sulphur appeared, and thermal decomposition (TGA/DSC), where the thermal stability of both catalysts was proven up to 250 ^{o}C. According to the nitrogen adsorption analysis, the surface area of the catalyst was found to be 50,416 m^2/gm for both the direct and reflux methods, respectively. FT-IR spectroscopy showed that the SO_2 and CH aromatics and aliphatic were clearly shown in FT-IR. As well as the scanning electron microscope (SEM) and the transmission electron microscope (TEM), which show the topography, size, and arrangement of the particles of the catalyst. The X-ray diffraction results for both catalysts showed the appearance of a wide band at an angle of 22^{o}, which proves that the surface is amorphous.

Cellulose and glucose decomposition were carried out over the prepared catalyst. Pyridine sulfonic acid homogeneous catalyst needed only 6 h to decompose 98% of cellulose to glucose. RHAPSA@Dir needs 9 hours to decompose 55% of cellulose. About 86% of glucose was decomposed in 4 h over RHAPSA@Dir. RHAPSA@Ref needs 10 h to decompose 41% of cellulose and 4 h to decompose 80% of glucose. According to our results the catalytic activity of the catalysts used in the decomposition of cellulose and glucose was followed the sequence below:

Pyridine sulfonic acid > RHAPSA@Dir > RHAPSA@Ref

Chapter One

Introduction

1.0 Introduction

1.1 Biofuel

In light of the rapid increase in demand for resources and the subsequent depletion of fossil fuels, there has been a worldwide push to develop and employ renewable energy sources[1], [2]. There are promising future prospects for the use of biomass as an alternative energy source [3], [4]. As a result of its ability to both replace fossil fuels and fix inorganic carbon through photosynthesis, solar power has the potential to significantly reduce carbon dioxide emissions [5]. Lignocellulose, one type of biomass resource, has attracted a lot of interest because of its potential to alleviate global food shortages and its ease of production. Most lignocellulose is made up of cellulose, a major natural polymer and an important renewable material source for the chemical industry [6]. Nanocellulose has been isolated in a number of distinct forms from cellulosic feedstock [7]. Nanocellulose materials have several potential applications in various areas of human life [8].This discovery opens up a new avenue for addressing a wide range of water pollution challenges. Glucose, 5-hydroxymethylfurfural (HMF), and levulinic acid (LA) are only a few of the energy molecules and platform chemicals that can be extracted from cellulose hydrolysis [9], [10]. Bioethanol production benefits greatly from the use of glucose, and HMF can be converted to low-oxygen diesel fuel from carbon 9 to carbon 11 [11]. LA has emerged as a promising feedstock for the production of liquid fuels [12] due to its ability to serve as a chemical bridge between the processing of biomass and petroleum. In addition, LA was recognized in 2004[13] as one of the most productive compounds derived from biomass that adds value. The synthesis of LA from cellulose is a topic of active research in the field of highly valued biomass conversion [14]. In recent years, there has been a meteoric rise in the manufacturing

and use of biofuels. Fuel ethanol output has more than doubled in the last four years, from 31.3 billion littres in 2005 to over 72.8 billion litters (estimated) in 2009 [15] .With Brazil and the United States at the forefront of this trend. The generation of renewable fuels in the United States is evidenced by the ongoing success of the fuel ethanol business. The Biofuels Digest [16] reports that in 2007, the United States was able to produce 7.5 billion litters of ethanol, an increase of 40% from 2006. In 2008, the country's ethanol production capacity grew to 13.3 billion littres. According to the study by Kim and Dale (2004), 40% of all crop leftovers can be used for biofuel generation[17]. All residues except rice straw and sugarcane bagasse can be eliminated. natural material that can be replenished and uses the sun's rays to produce energy [18]. Because it can be grown in vast quantities for far less money than crops that produce starch (like corn) or sucrose (like sugarcane), it holds considerable promise as a source for cheap fuel ethanol. Carbohydrate polymers comprising finite carbon (SC) and six carbon (6C) sugar units make up the majority (50–80%) of lignocellulosic biomass on a dry basis. Biofuels can be produced through the chemical or biological processing of most carbohydrates. Obtaining a fermentable hydrolysate rich in glucose from the cellulose content of the feedstock is essential to the use of lignocellulose for ethanol production. Enzyme use in lignocellulose hydrolysis is seen as the most promising approach since it has the potential to outperform other chemical conversion routes in terms of yield, by-product generation, energy consumption, mildness of operating conditions, and environmental friendliness [19].

1.2 Cellulose

Engineering, scaffolding, pharmaceuticals, fibre media, nano sensors, and glue are just a few of the many uses for cellulose [20]. Fig.1.1 depict the cellulose

molecule's composition. Agriculture residue, water plant grasses, straws, and other plant substances all contain cellulose because the polysaccharide is thought to be the primary constituent of the wall of the cell of the plant [21]. Wood, hemp, cotton, and linen all come from trees, which are the natural source of cellulose [22]. The molecular formula for cellulose is $(C_6H_{10}O_5)$ n, where n is the number of repeating glucose units [23].

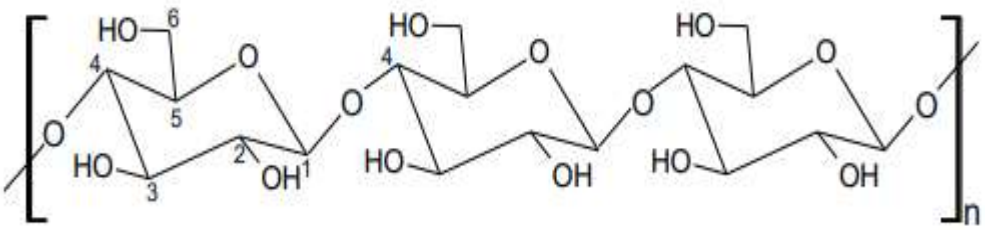

Figure 1.1: Structure of cellulose [24].

Cellulose, which makes up roughly 40–50% of the lignocellulose biomass cell wall, is a linear and homopolymer made up of D-glucose units connected by β-(1-4) glycoside bonds [24]. Glucose is swapped out for cellobiose in the repetitive stereochemical units of other glycan polymers [25]. Cellulose fibres are held together by hydrogen bonds, covalent bonds, Van der Waal forces, and each fibre contains anywhere from 20 to 300 microfibrils [18]. Linearity of homopolymer chains is determined by hydrogen bonds inside microfibrils, while amorphous/crystallinity of cellulose is determined by hydrogen bonds between strands [26]. Enzymes biosynthesize cellulose chains, which are deposited constantly and eventually aggregate into microfibrils. On a larger scale, the microfibrils join together to create fibres [27]. All plants are not created equal when it comes to their cellulose composition. Cotton has the highest cellulose concentration (90–99%), followed by wood (40–50%), jute (60–70%), and flax fibres (80%) [28].Most of the time, repeating units of as few as 20 can cover the full range of cellulose properties. The

initial C4-OH at one end of a cellulose chain is known as the non-reducing end. Chemical treatments, such as bleaching compounds, can add carbonyl and carboxyl groups to cellulose. The molecule structure is responsible for many of the material's distinctive characteristics, such as its hydrophobicity and degradability, relative thermostabilizing, high sorption capacity, and modifiable optical appearance [29]. Organic water-free fluid systems typically consist of one, but can have up to three individual components. The most probable crucial step is the pre-activation of cellulose to a soluble state. N,N-dimethylacetamide/lithium chloride (DMA/LiCl) and 1,3-dimethyl-2-imidazolidinone/lithium chloride (DMI/LiCl) are examples of popular two-component liquid systems [30]. Hello et al. (2014) recently introduced a new solvent system to dissolve cellulose. DMF/LiCl and cyclohexanol/LiCl are two systems that have shown great promise for dissolving cellulose [31].

1.3 Hydrolysis of cellulose

The process of hydrolyzing cellulose with an acid, enzyme, or other catalyst, which may be attenuated or highly concentrated. Cellulose hydrolysis has emerged as a major technology for the active use of lignocelluloses. This is due to the fact that glucose may be easily condensed into a variety of chemical biofuels, meals, and medications [32]. As the first step in many biorefinery processes, cellulose hydrolysis is crucial to sugar-based chemical and biochemical industries like the ethanol fuel industry. Cellulose is a renewable carbon source, but its recalcitrant structural which account a difficulties recyclable source for scientists.The breakdown of cellulose by enzymes, acids, and supercritical water has been the subject of extensive research [33].Changes and zangabao [34] , have been studied as acid-catalyzed hydrolysis through breaking hydrogen bonding and the -1,4 glycosidic bond Ionic liquids have been employed to form homogenous solutions through

hydrolysis of cellulose prior to hydrolysis. Scheme 1.1 shows the hydrolysis of cellulose by solid acid.

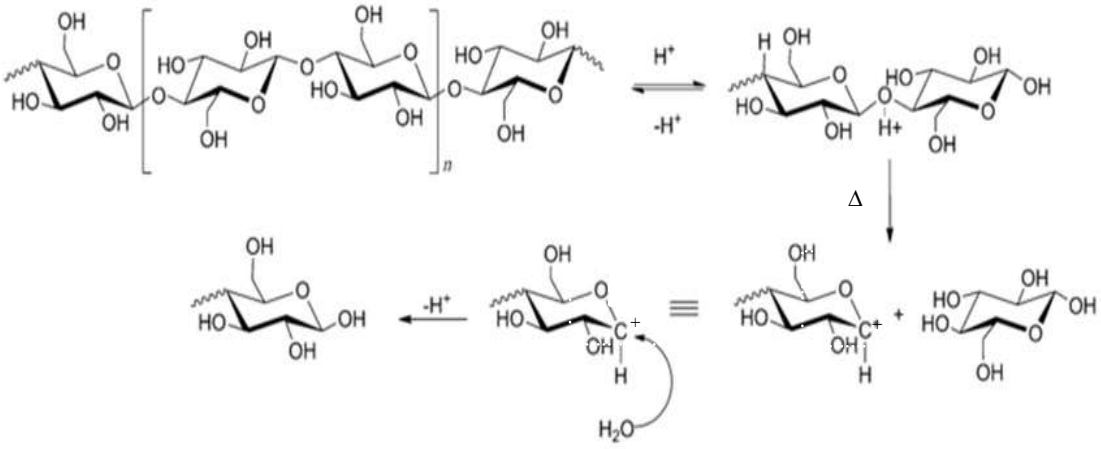

Scheme 1.1: Solid acid- catalyst hydrolysis of cellulose to form glucose [34] .

Acid hydrolysis is the most common method for converting cellulose to glucose because H^+ ions penetrate cellulose molecules, initiating breaking of the glycosidic bond (β-1,4). The success of the hydrolysis reaction was highly dependent on the parameters under which the reaction took place (i.e., the type of acid used, the amount of acid used, the length of hydrolysis time, and temperature[35]. Native cellulose strands are hydrolyzed by sulfuric acid, resulting in the fragmentation of the fibre into rodlike shapes. Sulphate groups are introduced during hydrolysis by esterifying surface hydroxyl groups, resulting in a stable water suspension of these highly crystalline cellulose needles [36]. In Table 1.1, a number of different cellulose decomposition techniques used by another researcher.

Table 1.1. Hydrolysis of cellulose to glucose by different catalyst.

Catalyst	Tem. °C	Time h	Method	Glucose yield%	Solvent	Ref.
H_2SO_4	285	12	Liquid acid hydrolysis	90.8	Water	[37]
Ru/AC-SO_3H	245	5	Liquid acid hydrolysis	50	Water	[38]
AC-SO_3H	100	3	Liquid acid hydrolysis	64	Water	[39]
$PrSO_3H$-SiO_2	110	4	Liquid acid hydrolysis	63	Water	[40]
SUCR-SO_3H	120	24	Solid acid hydrolysis	55	Water	[41]
CoFe-SiO_2-SO_3H	150	3	Solid acid hydrolysis	7	Water	[42]
SPS-DVP-SO_3H	190	8	Liquid acid hydrolysis	48	Ionic liquid	[43]
H_3PO_4	190	6	Liquid acid hydrolysis	65	Water	[44]
Tungsted Aluminum	190	24	Liquid acid hydrolysis	42	Water	[45]
CP-SO_3H	110	10	Liquid acid hydrolysis	93	Water	[46]
P-toluene Sulfonic acid	160	3	Liquid acid hydrolysis	30.3	Water	[47]
Fe_2O_3-SBA-SO_3H	130	2	Liquid acid hydrolysis	50	Water	[48]
Silica with Zr, $TiO_2Al_2O_3$	160	12	Novel silica Catalyst thermal Condition and ball milling	50	Water	[49]
Fe-GO-SO_3H	75	9	Liquid acid hydrolysis	50	Water	[50]

Some examples of the kinds of chemicals that might result from the chemo catalytic hydrolysis of cellulose using different chemical techniques are shown in Scheme 1.2 [51]. Fuels that come to mind, among many others, include ethanol, hydrogen, methane, and compounds. By catalysing the change of lignocellulose biomass, substances like levulinic acid, glucose, sorbitol, fructose, and lactic acid could be manufactured. Syngas can be made from lignocellulose biomass, and the by-products of this process (carbon monoxide and hydrogen gas) can be used to make an array of useful compounds and fuels.

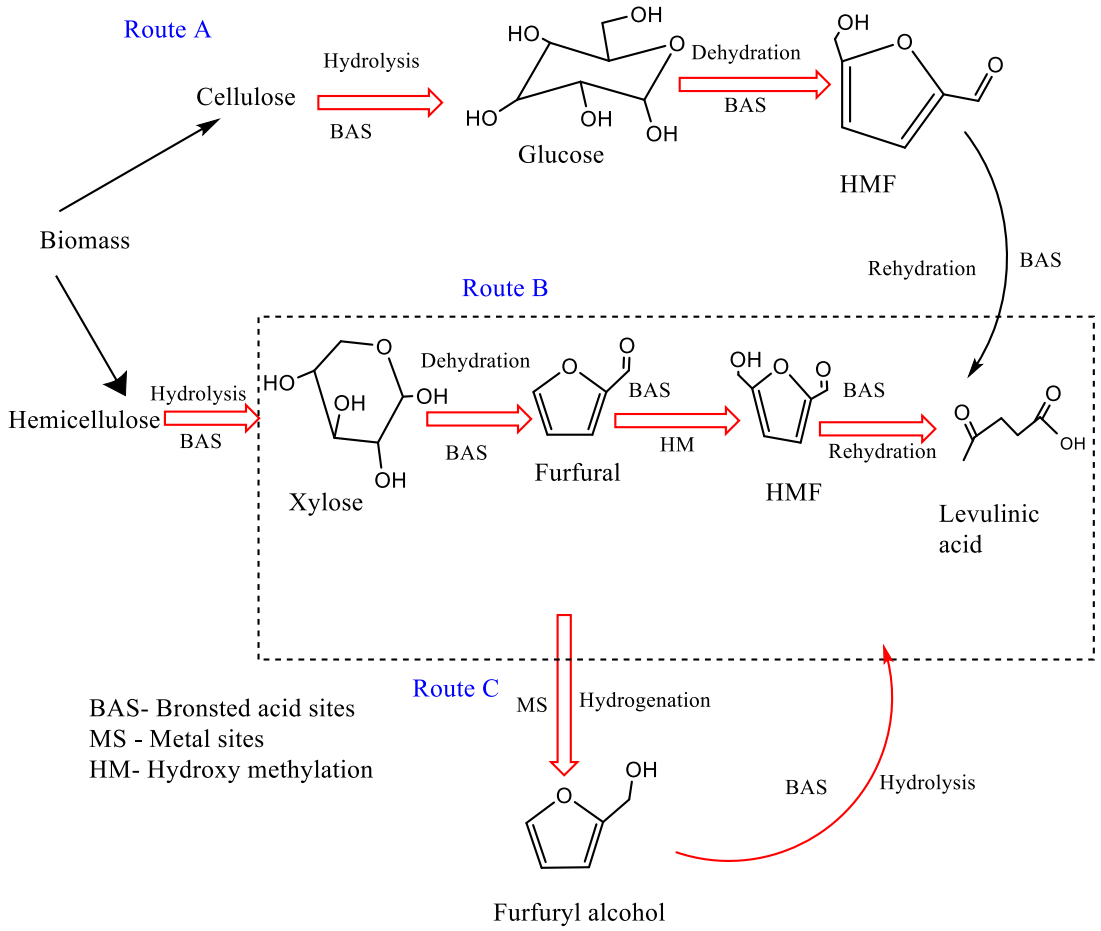

Scheme 1.2: Employing several catalysts to convert cellulose into glucose [51].

1.4 Homogeneous and heterogeneous Catalysts

Homogeneous catalysis refers to catalysis performed in a solution with a soluble catalyst. To be precise, a homogeneous catalyst is one that occurs in the same phase as the reactants during the catalytic process. Gas phase and liquid phase reactions are both suitable for homogeneous catalysis. In contrast to heterogeneous catalysis, heterogeneous catalysis involves catalysis that occurs in various stages of a reaction at the same time, such as the solid-liquid, solid-gas, and liquid-gas phases. The presence of distinct phases in the process distinguishes heterogeneous catalysts from homogeneous catalysts. When reactants chemisorb on a solid surface, for example, the weakening of internal bonds allows new bonds to be formed with other molecules; this sort of catalyst is heterogeneous and happens in a distinct phase from

the reactants and products [52]. Desorption, or release into the liquid phase, necessitates a decrease in the product's affinity with the catalyst [53]. Heterogeneous catalysts are highly sought after because of their ability to facilitate the creation of continuous chemical processes by allowing for simple isolation of the catalyst from the final product. Since heterogeneous catalysts may work under more extreme conditions than their homogeneous counterparts, the field of heterogeneous catalysis has never been more relevant. Not only is heterogeneous catalysis important because it is employed in so many industrial processes, but it is also garnering renewed interest as a result of widespread worries about energy generation and conversion, alternate energy sources, and climate change [54] .While both homogeneous and heterogeneous catalysis can be used to speed up various reactions, heterogeneous catalysis typically results in less waste, uses fewer toxic reagents, and makes the catalyst more easily retrievable and recyclable[55] .

1.5 Rice husk

Rice is the second most consumed food product in the world. With a growing population comes a need for more rice. Rice paddy production is dominated by China and India, which together account for around 48% of the world's total production. Around 20% of a bag of rice's total weight is made up of the rice husk RH, which is a by-product of industrial rice processing. Since it has a high calorific value (16,720 kJ/kg), most of it may be burned in boilers to generate energy. Rice husk ash (RHA) is a by-product of RH burning that contributes to pollution and disposal problems and accounts for around 20% of the weight of the husk itself Fig.1.2. About 200 kilograms (20%) of RH are produced from every thousand kilograms (1000 kg) of paddy grain, and when this grain is burned to provide energy, another 200 kilograms (20%) of RHA are produced, with a volume containing

approximately (85-95%) amorphous silica [56]. Both the environmental conditions and the technique used to burn the husk have an impact on the final product, which in turn affects the RHA qualities. Since it contains a lot of silica in its amorphous state, it can be used in many different kinds of manufacturing, including ceramics, construction, chemicals, and electronics. Due to the potential benefits of this area of RHA applications, many research have been done[57] .

Figure 1.2: (a) Rice plant, (b) Rice husk after removing of the rice**.**

1.5.1 Rice Husk components

Figure 1.1, RH is a by-product of the rice mill that accounts for roughly 20% of rice's total mass but is otherwise a waste product. Seventy-four percent of RH is made up of organic compounds such as cellulose, lignin, and hemicelluloses. Xylose, L-arabinose, methyl glucuronic acid, and D-galactose all combine to form hemicellulose. About 4% of the elements (Al_2O_3 + Fe_2O_3 + CaO + MgO) can be found in rice husk. It has tremendous potentials as a bio-sourced for industrial-scale

processing, making it a viable alternative to more conventional materials. Silica content in rice husk (RHA) is 95% when it is calcined at 600-700°C for 1 hour to 4 hours in a controlled environment (air or oxygen) [58].

Table1.2: RH chemical analysis [59] .

Constituent	Content (Wt.%)
Organic material and moisture	73.87
Al_2O_3	1.23
Fe_2O_3	1.28
CaO	1.24
MgO	0.21
SiO_2	22.12
MnO_2	0.074

1.5.2 Rice husk ash

Burning rice husks at a controlled temperature (500–800 °C) yields rice husk ash (RHA). Since RHA is produced as a by-product of RH biomass power plants, and landfills have limited capacity, disposal of RHA could pose serious environmental risks (as depicted in Fig.1.3). Amorphous silica, carbon, and a few other minerals make up the bulk of RHA. Many commercial and research uses for amorphous silica and carbon have been proposed [60]. Because of this, RHA can be employed as a low-cost replacement for amorphous silica in the manufacture of silicon-based products with technical relevance [61] .

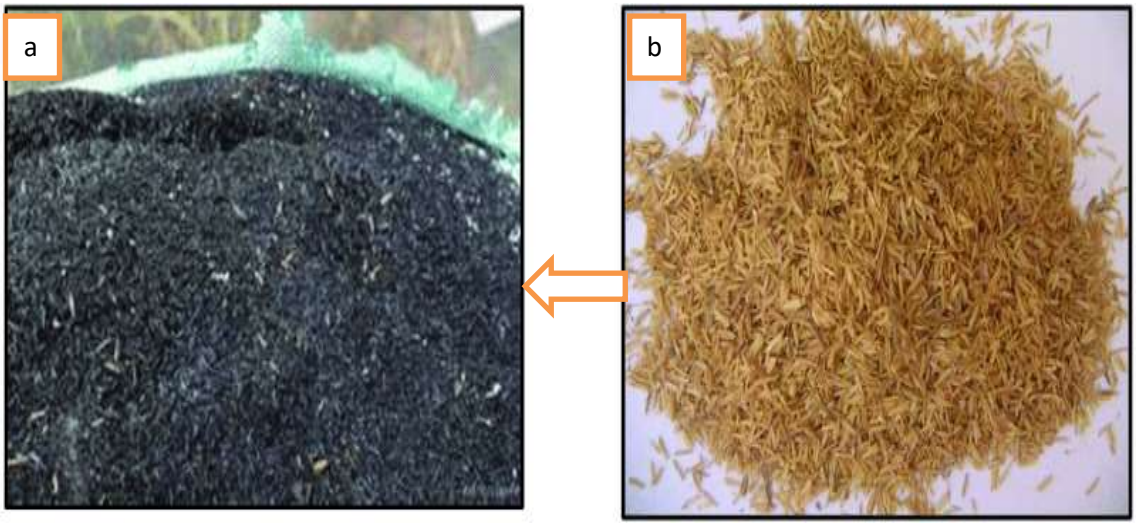

Figure 1.3: (a)Burned rice husk as waste material, (b) Rice husk [62] .

The ash contains mostly silica (94%) and other inorganic impurities (6%) [63]. The rice husk chemicals are listed in Tables 1.3. The term "RH ash" (RHA) is used to refer to any and all types of ash that can be made from RH. In actuality, the form of RHA obtained is considerably temperature dependent. At temperatures between 500 and 800 °C, amorphous silica is formed, while crystalline silica forms could be formed at higher temperatures [64] .

Table1.3: organic constituent of RH excluding silica [65] .

Constituent	Amount present in RH (Wt.%)
α-cellulose	43.30
Lignin	22.00
L-arabinose	6.53
Methyl glucuronic acid	3.27
D-xylose	17.52
D-galactose	2.35

1.5.3 Extraction of silica from rice husk

There are a number of techniques for silica extraction from RH. In Fig. 1.4, the many processes that can be following to convert RH into silica. Impurities are

eliminated before and after the heat phase in these procedures. The chemical approach, which comprises straightforward acid leaching, is among the most well-liked methods for obtaining SiO_2 from RH. To create SiO_2 nanoparticles from RH, post-annealing is widely regarded as one of the easiest and most effective methods of synthesis [66] .

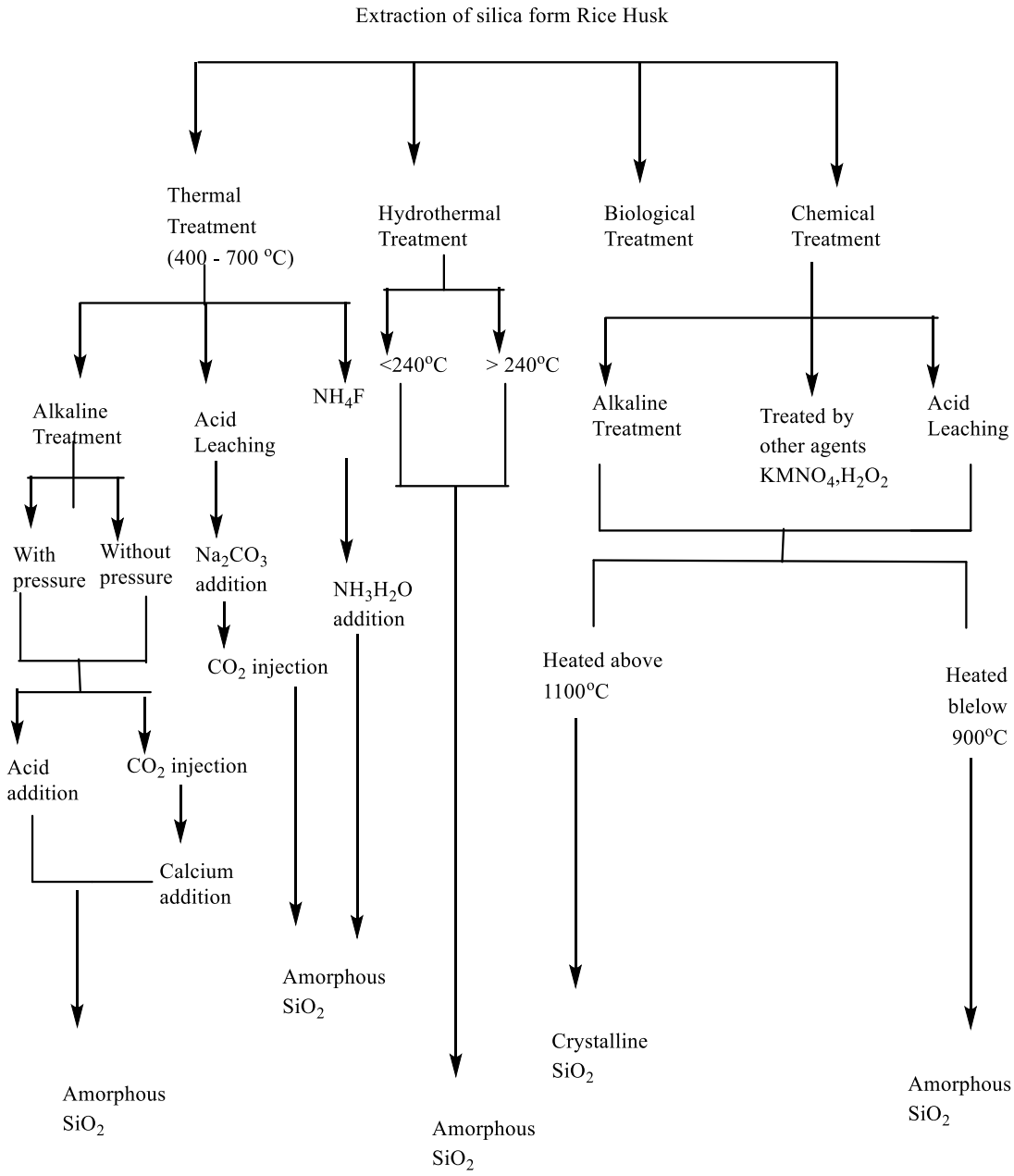

Figure 1.4: Different methods for silica extraction from RH [66] .

1.5.4 Structure of RHA

In order to learn more about silica, numerous researchers have examined it. A siloxane group (Si-O-Si) with oxygen on the surface, or one of several other forms of silanol groups, marks the surface termination of the structure (Si-OH). Silanol forms when an OH group is covalently bonded to a single silicon atom on the surface; vicinal silanol forms when two free silanol groups connected to different silicon atoms are close enough to the hydrogen bond to form a bridge. To establish a hydrogen bond, the two hydroxyl groups attached to the silicon atom in the third type of silanol, geminal silanol, are too near together[67] see Fig.1.5 (a, b, and c). Amorphous silica highly disordered surface structure makes it unlikely that hydroxyl groups will be arranged in a predictable fashion. As a result, the surface of amorphous silica can be covered in both free and bonded hydroxyl groups. Full coverage can be obtained if the surface is totally hydroxylated [68], whether the surface already has both forms or merely isolated hydroxyl groups (as in crystalline silica). When exposed to water, it can also physically absorb water through hydrogen bonding. When the partial pressure is raised, a multilayer of adsorbed water forms on the surface of a totally hydroxylated, nonporous silica species. Subsequent capillary condensation then occurs on the adsorbed multilayer, and the pore volume gradually fills with liquid water. Hydration refers to the process of consuming water through physical absorption [69] .

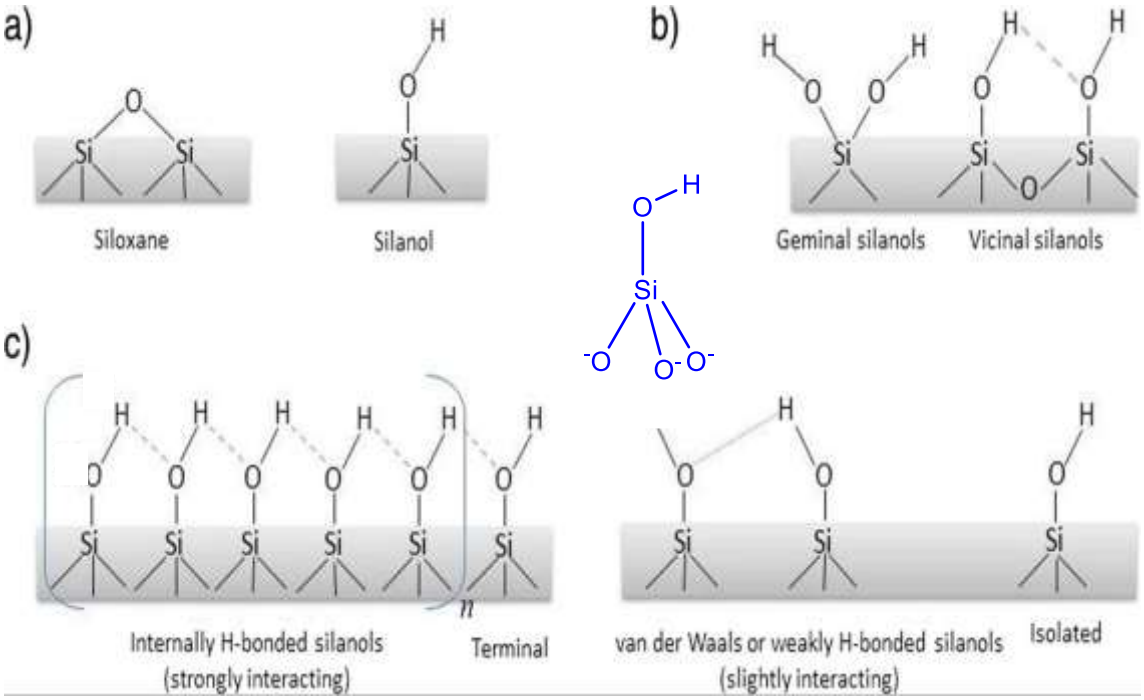

Figure 1.5: Different types of silanol group in surface of silica [70].

According to the NMR data, there are three distinct siloxane groups (=Si-O-Si=), each of which can be written as Q=Si (OSi)n (OH)4-n, where n = 2-4 to denote the number of bridging bonds (O-Si) linked to the central Si atom (e.g., Q^2, two siloxane linked to the central Si atom). Q^3 has three silicon bonds for each core silicon atom. Q^4, having four siloxane linkages connecting each centre silicon atom. As Fig. 1.6 demonstrates, in addition Three distinct types of silanol groups have been observed on the surface of silica during experiments: the isolated silanol group, in which each silicon atom is linked to a single hydroxyl; the vicinal silanol group, in which one silanol group forms an intermolecular hydrogen bond with another silanol group; and the geminal silanol group, in which two hydroxyls are bonded to a single silicon atom, yielding the formula Si By reacting the silanol functional group with an organic nucleophile, the silica surface can be activated to form new bonds (≡Si-O-C =, ≡Si-O-C ≡) [71] .

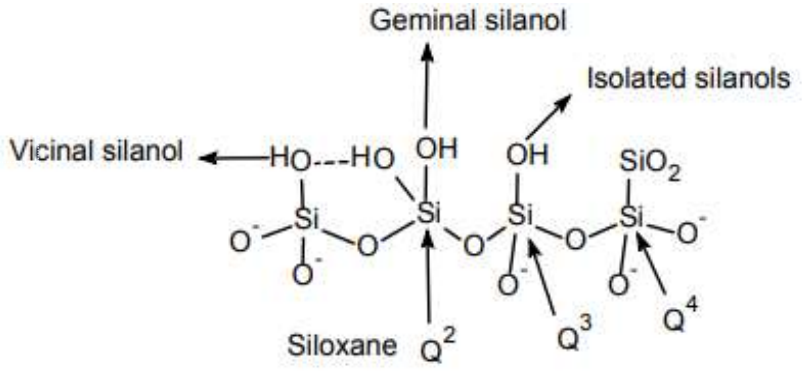

Figure1.6: Various type of silanol and siloxanes group on the matrix of silica [71].

1.6 Surface modification of silica

The addition of superficial functional groups via various modification techniques has a significant impact on the use of silica materials [72].There has been a lot of focus on surface modification of silica since it allows scientists to change the composite material's chemical properties and technological qualities. The surface of silica must be modified in order to create crucial materials with numerous specialized qualities, such as liquid crystals, nanostructured silica materials, and selective heterogeneous catalysts [73].When alkyl silanes are used for surface modification, the role of the surface silanol group is crucial [74]. The silanol groups on the surface of silica are dehydrated as the temperature rises, and the dehydration of these groups eventually leads to the creation of a siloxane bond [75]. According to the diverse approaches to incorporating the silica component into the silica-based hybrid nanostructures, the production of silica-based nanomaterials with well-defined topologies can be broadly divided into two categories [67]. The First method involves a heterogeneous reaction between the silylating agents and the ligand complex, as shown in Scheme 1.3. Followed by immobilization of the resultant ligand with the pre-formed silica. The second method, depicted in Scheme 1.3 entails introducing a complicated group after the post-polysiloxane.

Certain organic processes can lengthen the organic chain that forms when a particular alkoxysilane is bound to an inorganic support, leading to an increase in the number of additional basic centers on the surface [76] .

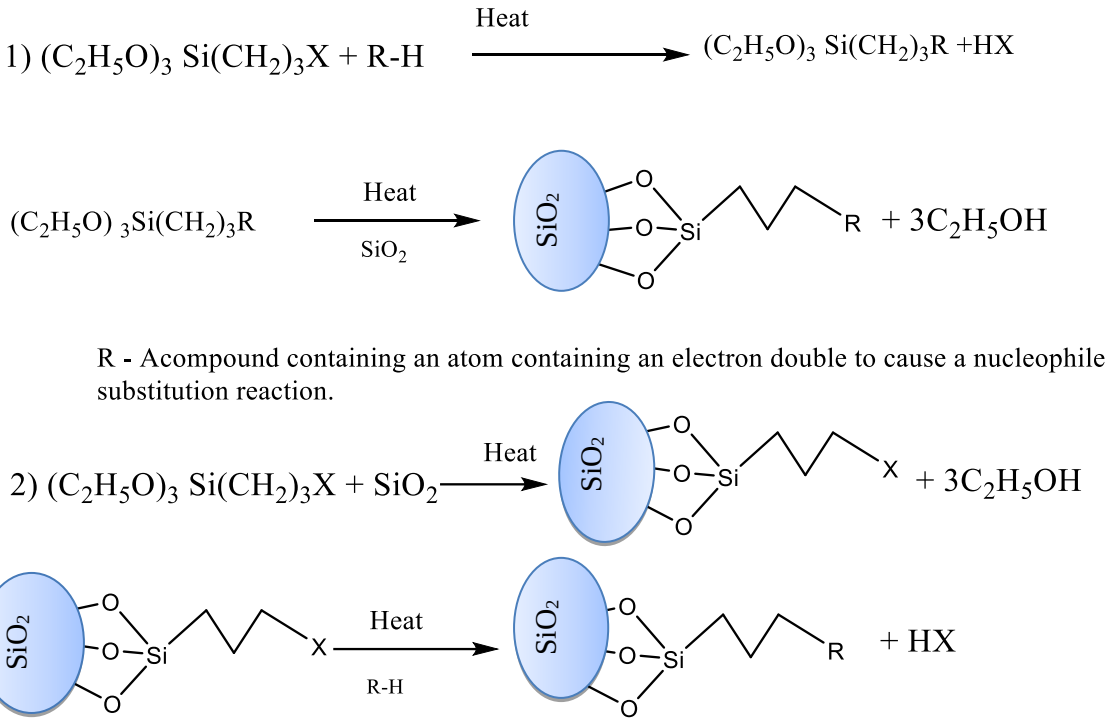

Scheme 1-3: The resulting ligand can be immobilized on silica following the reaction between the ligand complex and the silylating agent. Prior to immobilizing the ligand complex, the silylating agent is first applied to silica.

Several researchers have studied both of these methods thoroughly [31], [77]. The main drawbacks of these processes are the use of potentially harmful solvents and chemicals and the lengthy reaction times. This approach may lead to a nonuniform spread of these groups because they are primarily bound to the pore interior [78]. Moreover, these processes necessitated the use of toxic organic solvents, prolonged periods of reflux, and high temperatures [79]. Recently it was discovered that silica was capable to immobilized with CPTES via sodium silicate. High yields of silica

surface were modified in low-cost by-product of the rice grinding process. This procedure has been used to develop RHACCl in numerous experiments[80], [81] .

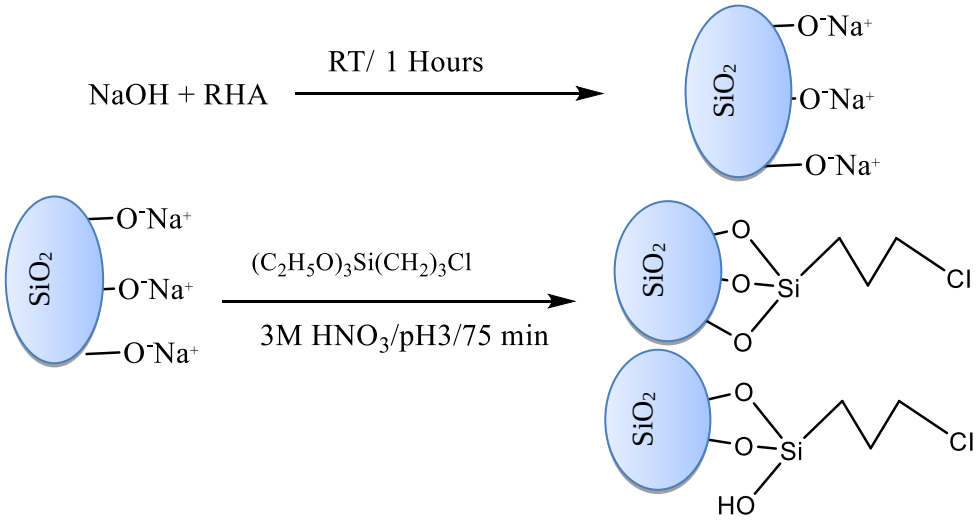

Scheme 1.4: Functionalized of silica with CPTES to produce RHACCl [80].

1.6.1 Silica – chloride end groups

The uses of organic amines and ammonium salts as heterogeneous catalysts have been proven to be extremely useful for many processes. It is a nucleophilic substitution reaction when a C-X (X= halogen) functional group reacts with a base organic molecule or ligand (such as an amine group) [82].Saccharine, also known by its chemical symbol Sac, is a common manufactured sweetener that functions as a secondary amine. The structure contains two types of hetero atoms—S and N. Because of the strained structure of the Sac molecule and the presence of lone pair electrons on these atoms, they may serve as catalytic sites that confer some selectivity. Coordination interactions with transition metals formed by these heteroatoms can be used in subsequent catalytic reactions and their catalytic activity in esterification reaction (Scheme 1.5)[83] .

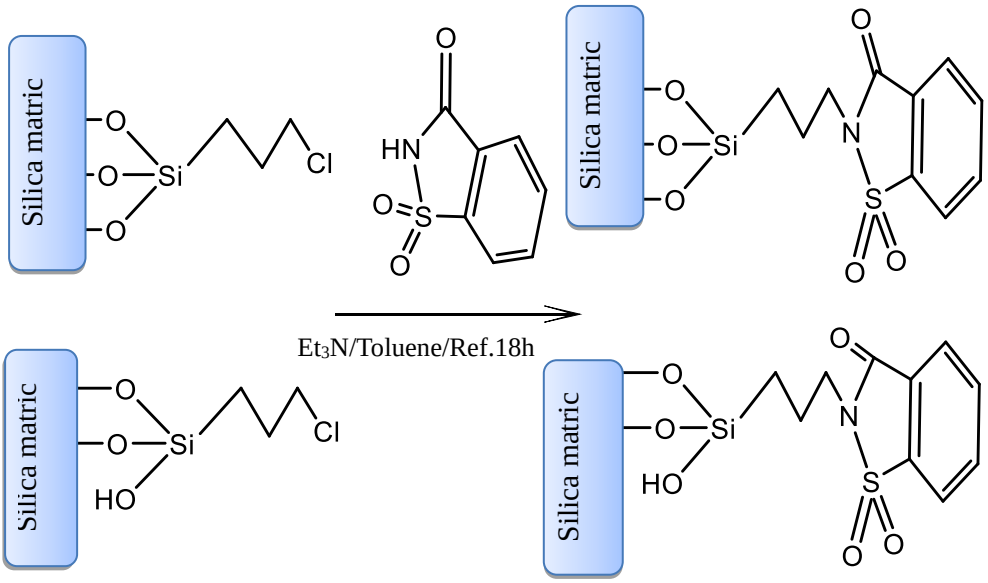

Scheme 1.5: The immobilization of saccharine on RHACCl. The preparation of (a)and (b) had been reported [83] .

Heterogeneous reactions were used to immobilize2-((2-phenylhydrazono) methyl) phenol (PHMP) on RHACCl. A heterogeneous reaction is one in which at least one of the reactants is in a non-equilibrium condition. To produce the final catalyst was shown in the scheme1.6. Dry toluene was used as the solvent, and the reaction combination was placed in a reflux oven for 44 hours to give the final goods depicted used hydrolysis cellulose in (Scheme1-6) [22].

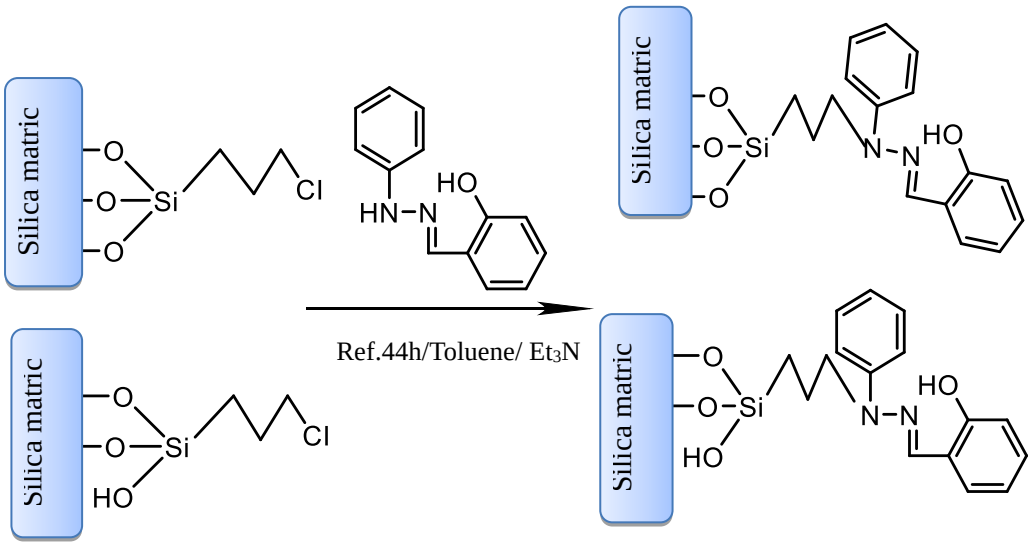

Scheme 1.6: The immobilization of PHMP on RHACCl.

Using silica-trapped N-heterocyclic carbenes (Scheme 1.7) [84] glycerol cyclization has been accomplished using the prepared catalyst. Condensation with aldehydes and ketones to produce cyclic acetals is one of the most noteworthy applications of glycerol. The cosmetic [85] pharmaceutical [86] and food and beverage sectors all find applications for these acetals, so they are considered valuable chemicals[87] .

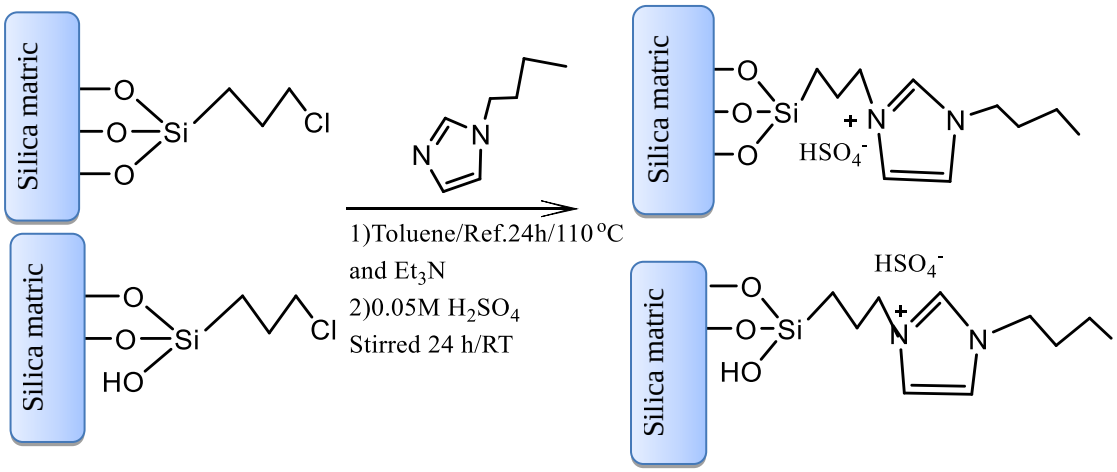

Scheme 1.7: A reaction between N-heterocyclic carbenes and Carbon – halogen silica functional group of preparation heterogeneous for glycerol cyclization reaction.

Scheme 1.8 showed the process of preparing a heterogeneous acidic catalyst by grafting sulfanilic acid onto RHACCl. In the process of alkylation, the catalyst was utilized, and it was discovered that it could be recycled numerous times without suffering any reduction in its capacity to catalyze the reaction [88].

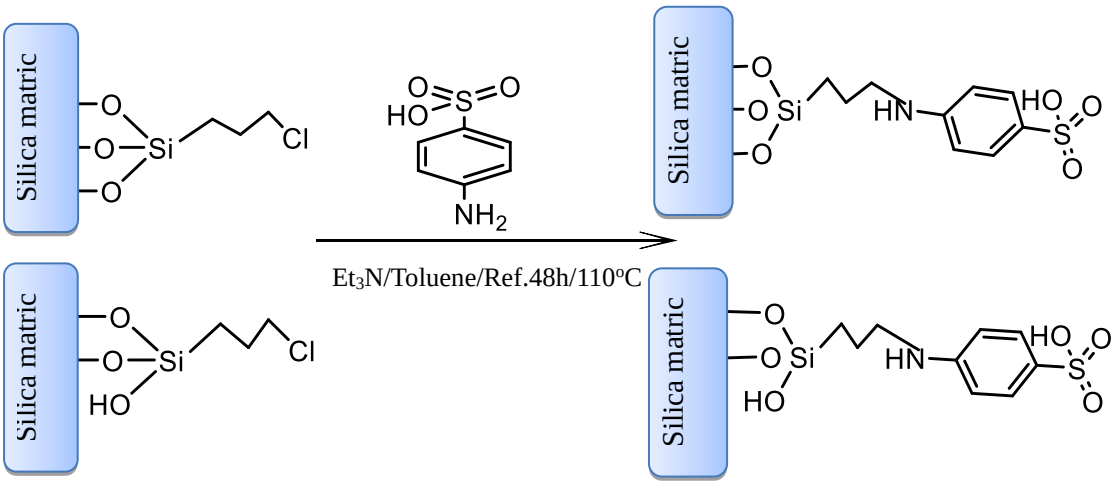

Scheme 1.8: The immobilization of sulfanilic acid with RHACCl.

RHACCl was used to treat dithiooxamide (DTO) and p-phenylenediamine (P-PDA) in dry toluene and Et_3N (Scheme 1.9). It was discovered that the catalyst functioned best when ethyl alcohol and acetic acid were esterified[89] .

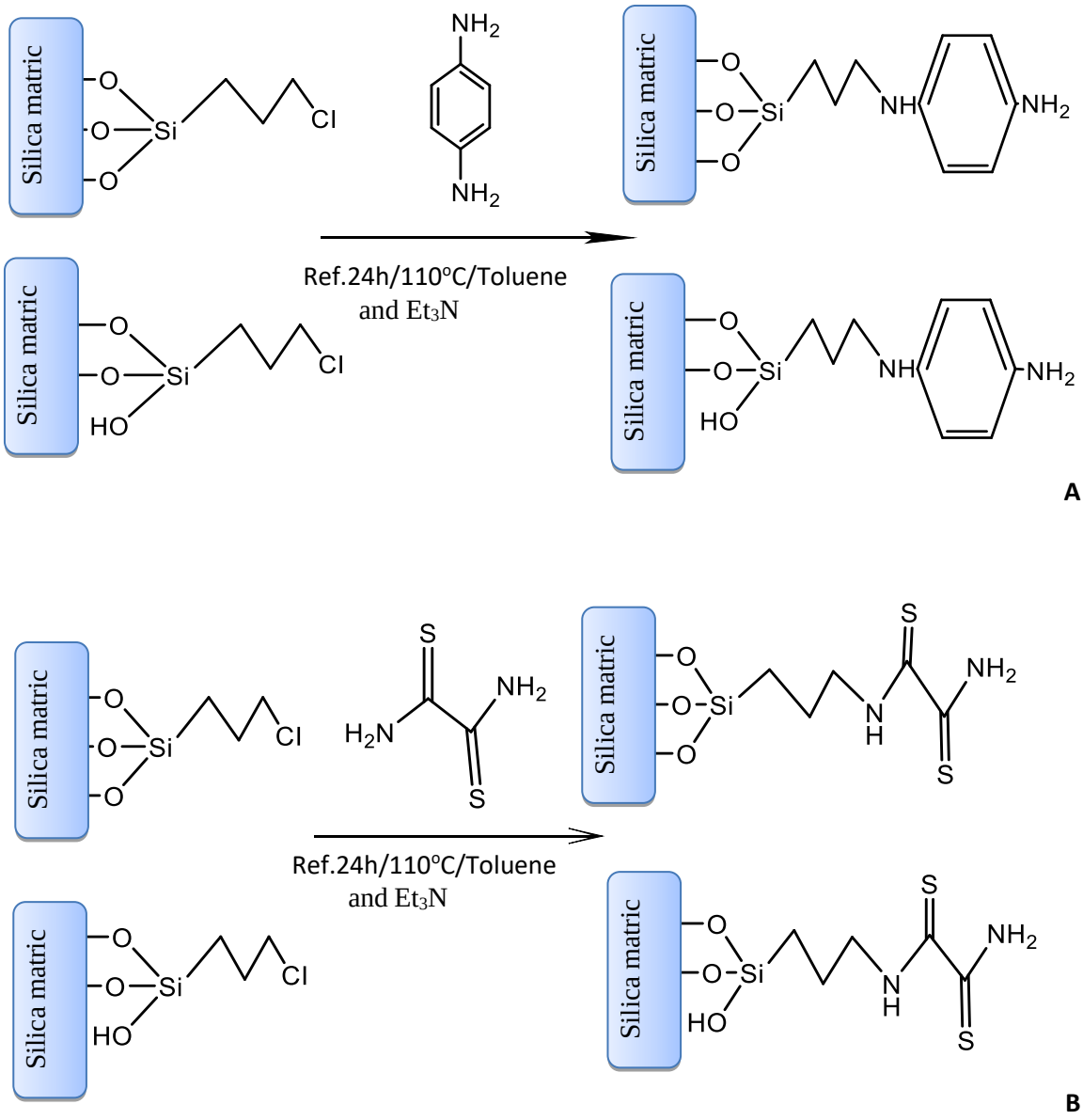

Scheme 1.9: The interaction of dithiooxamide and p-phenylenediamine onto RHACCl shown by (A, B) [89].

A nucleophilic substitution process between the chloride groups and urea took place. After adding urea (which contained amine end groups) to silica, sulphating it with

dilute sulfuric acid yielded a new solid-state catalyst for converting cellulose to glucose, designated RHAUR- SO4H [90] .

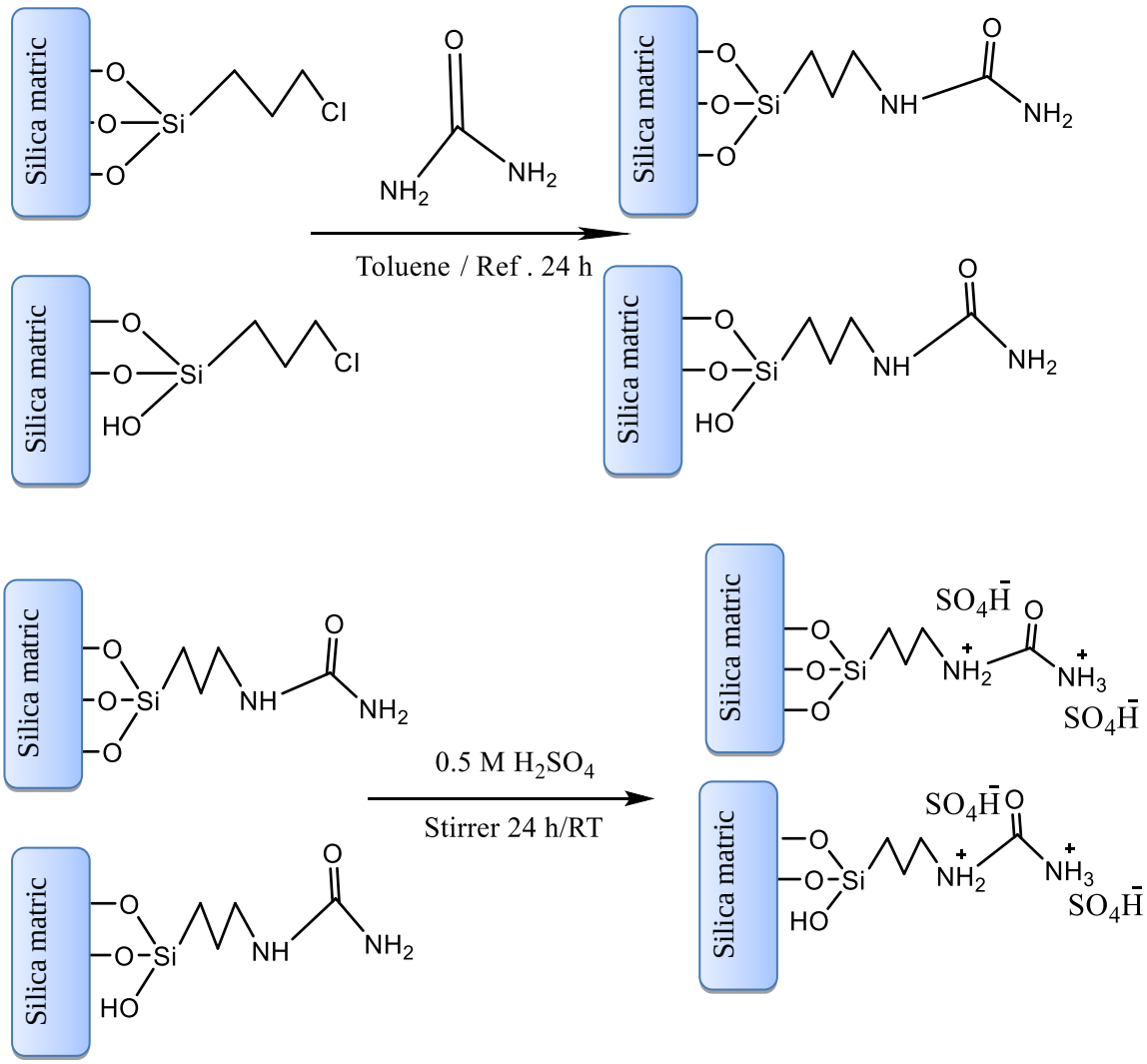

Scheme 1.10: The reaction between RHACCl and urea and sulphating with dilute sulfuric acid of preparation catalyst for hydrolysis cellulose.

1.7 The aims of the study

It has been known since 1640 that RHA contains silica, and that this silica can be removed by burring rice husk at 550-800 ℃ for 6 hours, after which a heterogeneous catalyst can be synthesised for different purposes. The target of this work are.

1- Extraction of the silica from rice husk.

2- Preparation of the heterogenous catalyst by simple direct modification of the silica with pyridine sulfonic acid and CPTES.

3- Preparation of the heterogenous catalyst by modification of the silica extracted from RHA with pyridine sulfonic acid by post modification in reflux methods.

4-Characterization of the prepared catalysts from the two methods by different spectroscopic and microscopic techniques, such as XRD, TGA, CHNS analysis, N_2 adsorption-desorption, FT-IR, SEM, and TEM.

5- A comparison between both catalyst by their characterizations and applications.

6- The catalysts using in the hydrolysis of cellulose to mono saccharide and in-situ hydrolysis of mono saccharide to other products.

7-To compare the hydrolysis of homogenous pyridine sulfonic acid with the heterogenous catalyst.

Chapter Two

Materials and methods

2.0 Materials and methods

2.1 Chemicals and instrumentals

All Items used in this thesis were not purified. It was used as in its form. Table 2.1 shows the items a long with their supplier and purity. Table 2.2 shows the equipment and its model with the place of analysis used in this study.

Table 2.1: Chemicals used in this study.

Item	**Suppler**	**Purity%**
Acetone	GCC-England	99
Butanol	Fluka, Germany	98
Cellulose	BDH,England	98
Cyclohexanol	Riedel-dehaen England	99
3-Chloropropyltriethoxysilane	Sigma- Aldrich	95
Dimethylformamide	Alpha Chemika	99
Dinitrosalycilic acid	Riedel-dehaen	99
Glucose	BDH,England	99
Lithium chloride	BDH, England	98
Nitric acid	System, Spain	69
Sodium hydroxide	System, Spain	99
Toluene	GCC,England	98
3-pyridinesulfonic acid	Sigma Aldrich	98

Table2.2: The equipment's and its model with the place of analysis used in this study.

Item	**Model**	**Place of analysis**
(TGA)/ (DSC)	STA1500.Germany	Tehran University, College of Science
Elemental analysis (C.H.N)	GmbH-vario EL, German	Tehran University, College of Science
FT-IR	Shimadzu-8400s, Japan	AL-Muthanna University, College of Science, Chemistry Department
N2 adsorption – desorption analysis	TriStarII plus Version 2.03	University of Kashan, College of Science
pH Meter	HNA 211 Ph Meter C-AI	AL-Muthanna University, College of Science, Chemistry Department
SEM analysis	Fesem Tescan Mira3 France	Tehran University, College of Science
TEM analysis	100KV Model: EM10C	Tehran university, College of Science
UV-Visible Spectrophotometer	Lambda 35, Japan	AL-Muthanna University, College of Science, Chemistry Department
X-ray diffraction (XRD)	Xpert High Score HAOYUAN	University of Kashan, College of Science

2.2 Catalyst preparation

2.2.1 Extraction of silica from rice husk

The technique mentioned in the reference [91] was followed to extracted silica form RH. Distilled water was used to clean RH from dust. For 24 hours the RH was dried at room temperature. Nitric acid (1.0M) 250 mL was mixed with 30 gm of clean rice husk for 24 hours at room temperature under a continuous stirrering. After being dried at 110 °C for 24 hours, the husk was finally ready for use. To achieve

complete combustion, it was calcined in a muffle furnace at 800 ℃ for 6 hours. A total of 8.2 gm of ash was collected. The ash was crushed up so that it could be used as a source of silica.

2.2.2 Functionalization of SiO_2 with CPTES

A solution of 1.0 M NaOH (100 mL) was heated with 3.0gm of SiO_2 for 60 minutes at 80 °C. Filtration was used to purify the sodium silicate by removing any impurities. The sodium silicate solution was mixed with 6.0 mL of CPTES. After that, 3.0 M nitric acid (1 mL/min) was slowly added to the solution while stirring was maintained at a constant speed. Below a pH of 11, white gel became visible. After the pH of the solution was determined to be 3, the container was covered and left out overnight at room temperature. A separation for six times per sample, distilled water was used in a centrifuge for 16 minutes, and acetone was utilized in the final wash. The material was then dried for 24 hours at 110 °C. A 4.8 gm of powder identified as RHACCl was collated [92] .

2.3 Preparation of silica – pyridine sulfonic acid in one pot synthesis RHAPSA@Dir

The sodium silicate was mixed with 6.0 mL of CPTES and 2.0 gm of pyridine sulfonic acid. A titration of the mixture agents (3.0 M) HNO_3 acid was done while the change in pH was monitoring to the end of reaction. The white gel had begun to form at pH 9. At pH 3 the titration was stopped and the gel was left aside and covered until the next day at room temperature. The separation was accomplished using a centrifuge for seven times at 4000 rpm for 15 min using distilled water for washing the sample. Acetone was used in the last wash. After that, the product was dried at 110°C for 24 h. The total weighted of catalyst was 5.0 gm.

2.4 Preparation of RHAPSA@Ref (reflux method)

The RHAPSA@Ref was prepared by adding 1.5 gm of pyridine sulfonic acid to a suspension of 1.5 gm of RHACCl in 30 mL of dry toluene. The reaction mixture was refluxed at 120 ℃ for 48 hours. The solid phase was than filtered and rinsed with distilled water. The solid sample 1.4 gm has been dried at 110°C for 24 hours.

2.5 Hydrolysis procedure

2.5.1 Cellulose hydrolysis

To the mixture of DMF\LiCl (20 mL\0.5 gm) and cellulose (0.18 gm) were added to 0.15 gm of catalyst maintaining a constant hydrolysis temperature of 140 ℃ for 13 hours. A bout 0.5 mL at the reaction mixture was taken each hour. It was poured 2.0 mL of deionized water along with 2.0 mL of both (2.0 N) NaOH and DNS. The solution was boiled for five minutes in a water bath. The DNS reagent was produced using a method described in an IUPAC protocol [93]. The same conditions were used to prepare and incubate a blank solution. The blank reagent's absorbance was deducted at 540 nm. To determine the concentration of glucose in the hydrolysis solution, a standard curve of glucose was used.

2.5.2 Glucose degradation over the catalyst

The catalyst and glucose (0.1 gm) were added to the DMF mixture (20 mL) The degradation temperature was fixed at 140^{o}C. Approximately 0.5 mL of the reaction mixture was with drawing each hour. 2.0 mL of both (2.0 N) NaOH and DNS, as well as 2.0 mL of deionized water, were added to the mixture. The solution was boiled for five minutes in a water bath. The blank solution was prepared and incubated using the same techniques. The absorbance of samble and blank was fixed

at 540 nm. The color was red for the first three hours, then start to turn orange at four and five hours, and finally turn yellow after six hours. This indicates a reduction in the glucose concentration with increase of the hydrolysis time.

2.5.3 Measurement of glucose concentration

Miller's DNS method [94] was used to measure glucose formed and glucose degraded. Various amounts of glucose were mixed into distilled water to make a 2.0 mL sample solution. 0.05, 0.1, 0.25, 0.5, 1.0, 2.0, 4.0, 6.0 and 10.0 mg/mL. DNS solution and 0.5 mL of 2.0 N NaOH were added to each test tube. The containers were then filled with 10 mL of distilled water. After 5 minutes in a hot water bath, the absorbance at 540 nm was measured. By graphing absorbance vs glucose concentration, a reference curve was created. The unknown signal in this histogram reflected the analyte concentration.

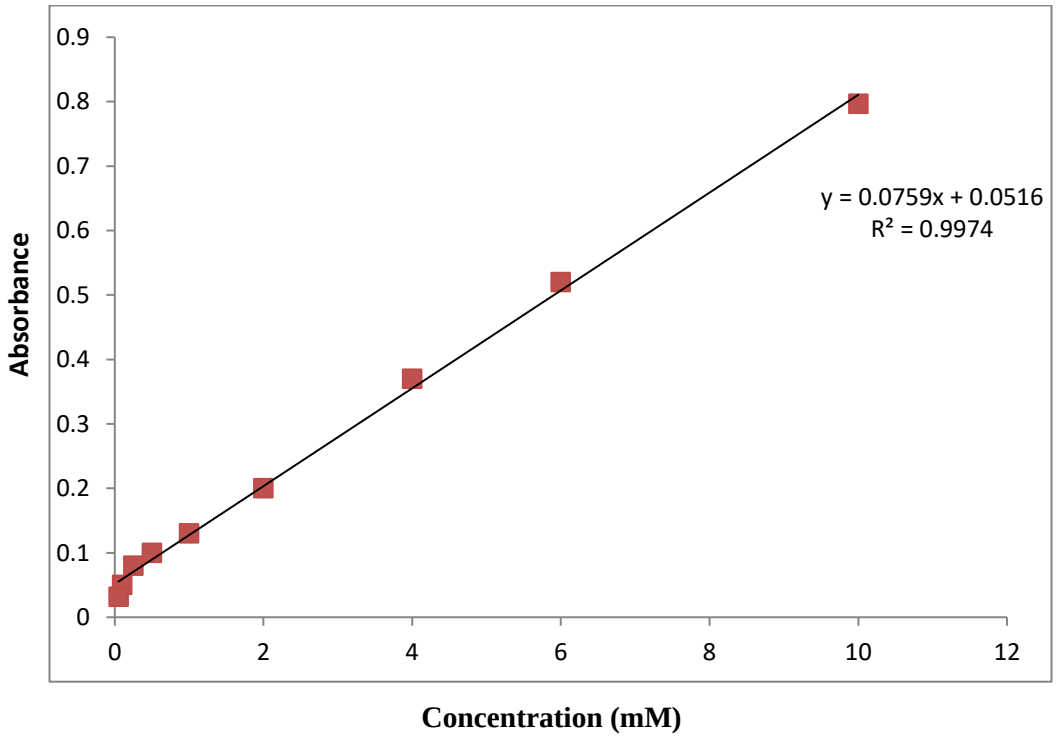

Figure 2.1: Standard curve of glucose.

2.6 The optimization of the catalyst parameters

2.6.1 Influence of catalyst mass

Using the same method outlined in section 2.5.1, the catalytic activity of various catalyst masses (0.05, 0.1, and 0.15 gm) was examined. The reaction was run for 13 hours at 140 °C and for glucose degradation the degradation was run for 10 hours.

2.6.2 Reaction temperature optimization

The method described in section 2.5.1 was utilized once again in order to investigate the catalytic activity at three different temperatures (120, 130, and 140 ^{o}C). The other parameters such as time, catalyst mass, and amount of cellulose or glucose were kept constant.

2.6.3 solvent effect

Investigation into the catalytic activity was carried out with a variety of solvents, including n-butanol, cyclohexanol, and toluene, using the same procedures as were detailed in section 2.5.1.

2.6.4. Recyclability of catalysts

To test the catalyst's reusability, the catalyst was collected after each run and classified as used for first time. After the initial hydrolysis with the new catalyst had finished the catalyst was filtered. A hot DMF used to wash, and dried of 110 °C drying. Under ideal circumstances, catalysts were reused in accordance with the technique described in sections 2.5.1 and 2.5.2 above.

2.7 Hydrolysis of Cellulose over homogeneous catalyst

In comparison, Cellulose hydrolysis using pyridine sulfonic acid as a homogeneous catalyst was performed in a liquid phase using a 100 mL circular bottom flask equipped with a magnetic stirrer and a water condenser. 25 mL of DMF, 0.18 gm Cellulose, and 0.5 gm LiCl were transferred individually to a round bottom flask containing 0.1 gm of pyridine sulfonic acid. The hydrolyses were carried out using a temperature of 140˚C and a reflux time of 13 hours. To 2.0 mL of deionized water, 0.5 mL of the clear hydrolyze solution was added in a vial. 2.0 mL of DNS reagent and 2.0 mL of 2.0 N sodium hydroxide were added to the solution before it was placed in a water bath heated to 90 ^{o}C for five minutes. UV-Visible spectroscopy was set to 540 nm to identified the presence of glucose.

2.8 Method of RHA Catalyzed Hydrolysis

Cellulose hydrolysis using RHA as a catalyst was studied using the same method described in sections 2.5.1 and 2.5.2. Both the hydrolysis and glucose degradation were carried out at 140 °C for 13 hours using 0.1 gm of RHA.

2.9 Method of Hydrolysis Using RHACCl Catalysts

Following the same protocol that was described in sections 2.5.1 and 2.5.2, the hydrolysis of cellulose employing a RHACCl catalyst was investigated. The Hydrolysis was performed with 0.1gm of RHACCl at 140 °C for 13 hours and for glucose degradation 10 hours was used as hydrolysis time.

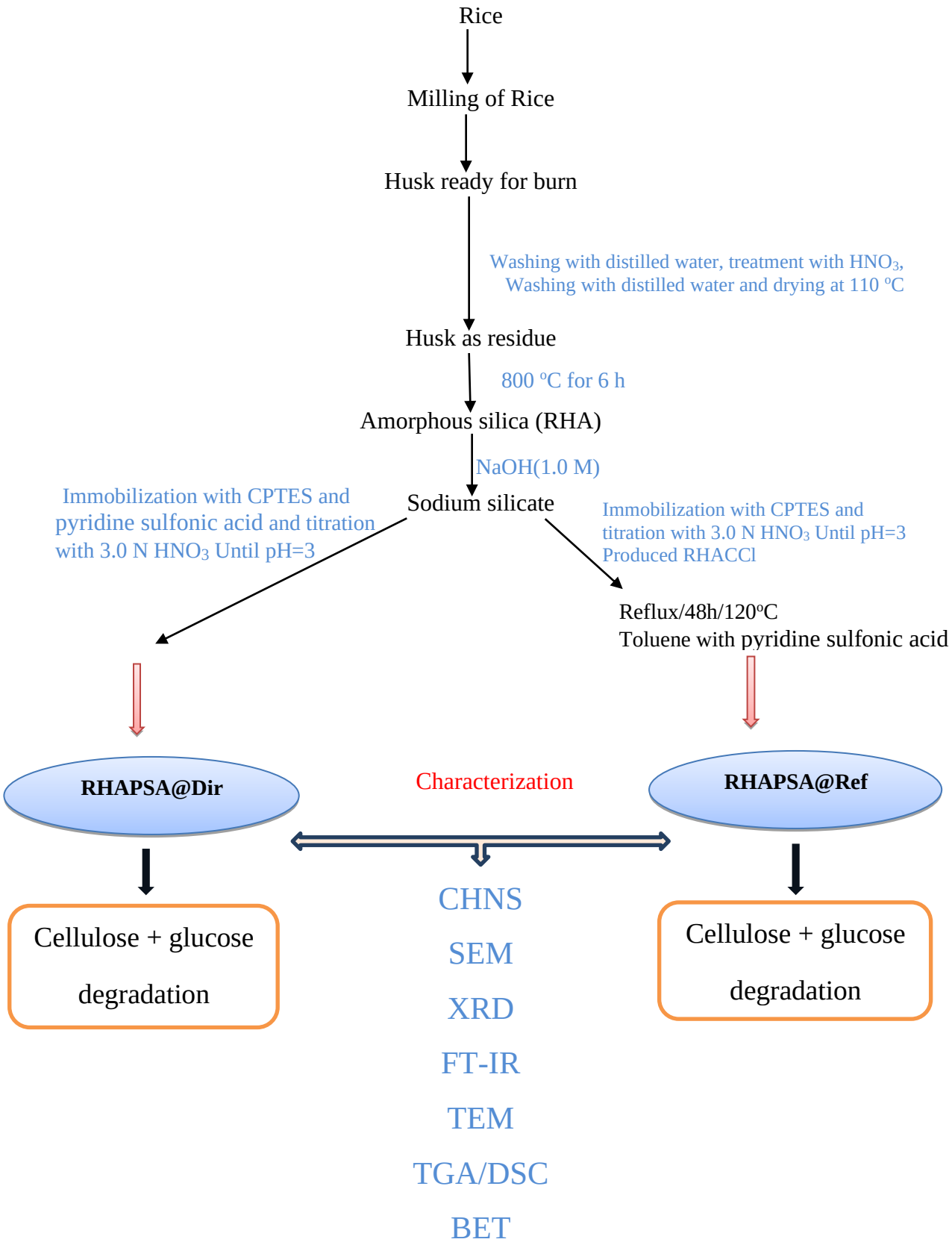

Scheme 2.1: Research diagram for catalysts preparation.

Chapter Three

Results and Discussion

3.0 Results and Discussion

3.1 Synthesis and characterization of RHAPSA@Dir

The sol-gel method was used to quickly and efficiently modify silica with CPTES and pyridine sulfonic acid in a single-pot synthesis that took only three hours. It was previously thought that silica reacted with CPTES to form silica-Si-$(CH_2)_2CH_2Cl$ end groups (known as RHACCl), and then the chlorine was replaced with PSA through in-situ transformation. Compared to conventional methods, which necessitate harsh reaction conditions and environmentally unfriendly solvents in addition to long reaction times and multiple steps. This procedure was performed under more favorable conditions during the reaction. When compared to this method, the yield from conventional techniques is interesting. Nitric acid "reverted" sodium hydroxide to a more natural form by exchanging the sodium ion for hydrogen. To functionalized silica with a ligand, the procedure was completely homogenous, with all reactants occurring on a single face of the material. The sequence of reactions for preparing RHAPSA@Dir is depicted in Scheme 3.1.

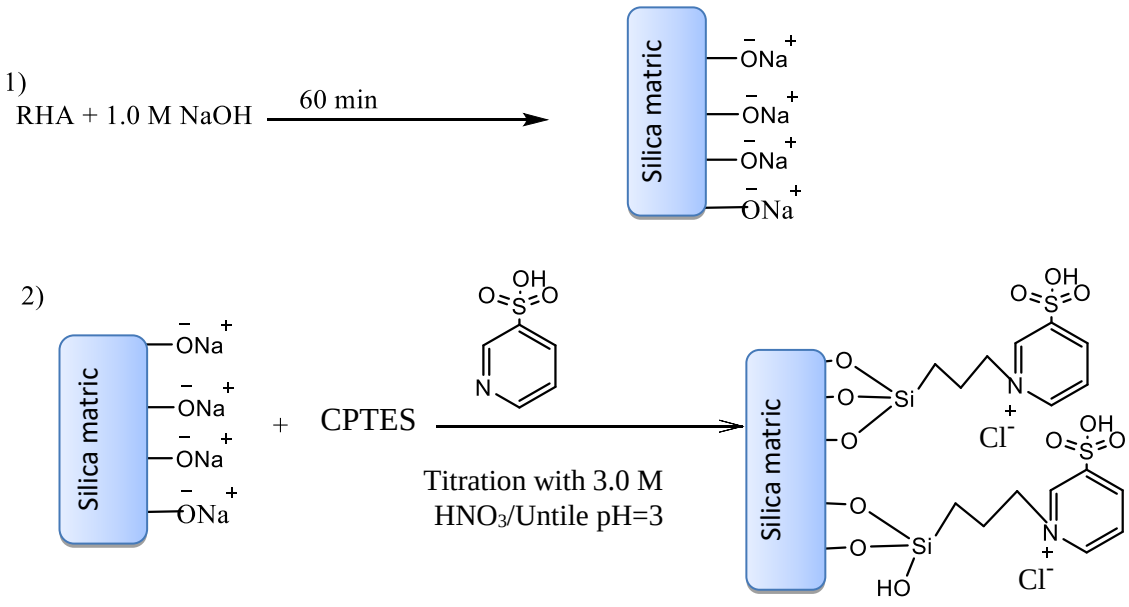

Scheme 3.1: This order reactions to produce a catalyst. After in-situ substitution of chloride with pyridine sulfonic, the resulting sodium silicate was transformed into propyl pyridine sulfonic-silica.

3.1.1 FT-IR spectral analysis

The FT-IR spectra of RHAPSA@Dir and RHA are shown in Fig.3.1. As shown in figure 3.1, the Si-O-Si absorption was determined at 1090 cm^{-1}. RHAPSA@Dir had an observed Si-O-Si absorption at 1068 cm^{-1}[95]. Broad band observed near 3464 cm^{-1} is typically attributed to O-H vibrations in SiO-H. At 3085 cm^{-1}, RHAPSA@Dir detects the aromatic C-H stretching vibration. The stretching modes of RHA did not display these bands. At 1453 cm^{-1}, the bending modes of the CH_2 group were appeared, including both symmetric and asymmetric vibrations. The C=C groups were responsible for the shoulder at 1634 cm^{-1}. RHAPSA@Ref spectra exhibit a band between 1306 and 1147 cm^{-1} due to SO_2 stretching bands. These results show that PSA nucleophilically substituted the -CH_2-Cl end group to generate RHAPSA@Dir [96].

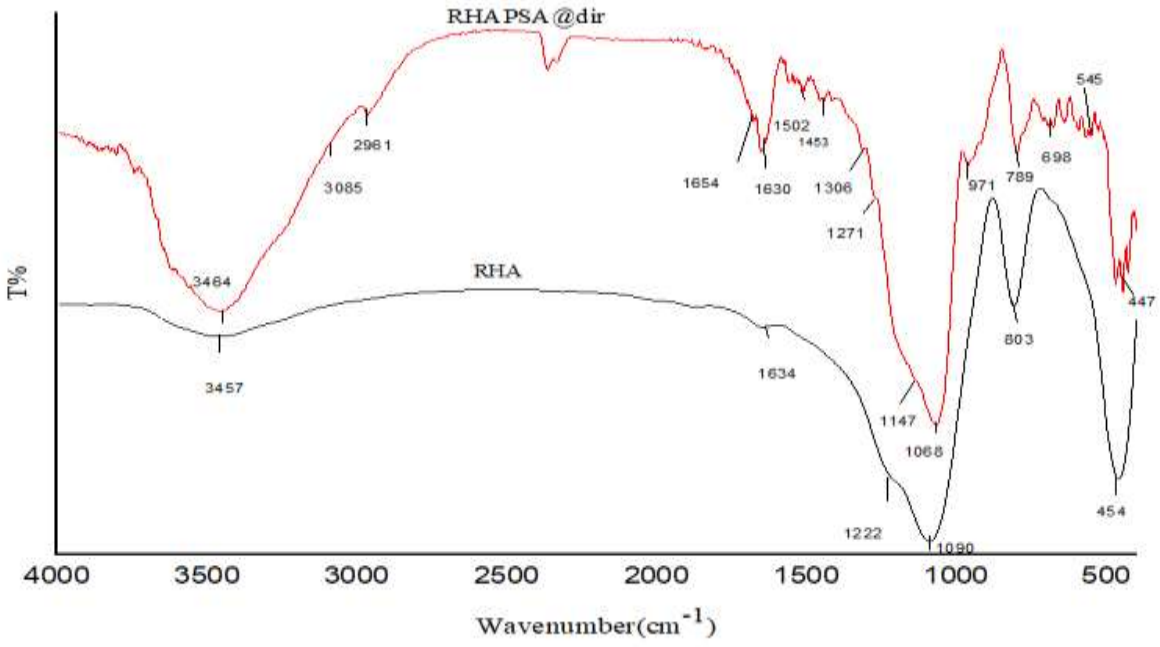

Figure 3.1: The FT-IR spectra of RHAPSA@Dir, and silica.

3.1.2 Elemental analysis (C.H.N.S)

Elemental data for RHA, RHACCl, and RHAPSA@Dir were listed in Table 3.1. The percentage of carbon in RHA was 0.42 % and 1.76 % of hydrogen [83]. RHACCl had 11.9 % of carbon and 1.91% hydrogen. RHAPSA@Dir showed 12.34% of carbon and 1.90 % sulfur and 0.81% Nitrogen. The presence of Sulfur and Nitrogen with the increased Carbon percentage indicated that pyridine sulfonic acid was incorporated into the silica structure.

Table 3.1: Elemental analysis data of RHA, RHACCl, and RHAPSA@Dir.

Sample	Elemental %			
	C	H	N	S
RHA [83]	0.42	1.76	-	-
RHACCl [92]	11.90	1.91	-	-
RHAPSA@Dir	12.34	2.01	0.81	1.90

3.1.3 TGA/DSC of RHAPSA@Dir

Fig.3.2 shows the results of TGA and DSC for RHAPSA@Dir. Three different decomposition stages were seen in the TGA/DSC graph of RHAPSA@Dir. Adsorbed water loss accounts for the initial drop in mass (around 2 %) from 34 ^{o}C to 129 ^{o}C. Decomposition of the pyridine sulfonic acid group bonded to the silica accounts (for 28%) for the second mass loss. At high-temperature silanol groups were aggregated, as seen between 600 and 900 ℃ (about 10%) [97].

The DSC curve (Fig.3.2) shows two exothermic and endothermic transitions, the first peak of which occurs between 50 and 125 ℃, with a maximum at 85℃. Loss of

absorbed water causes the initial exothermic shift. The second type of mass loss happens between 150 and 190°C, with a peak cantered at 160 °C. The third phase happens between 350 and 540 °C, whereas the other transformations were referring to the removal of the organic structure of the catalyst [90].

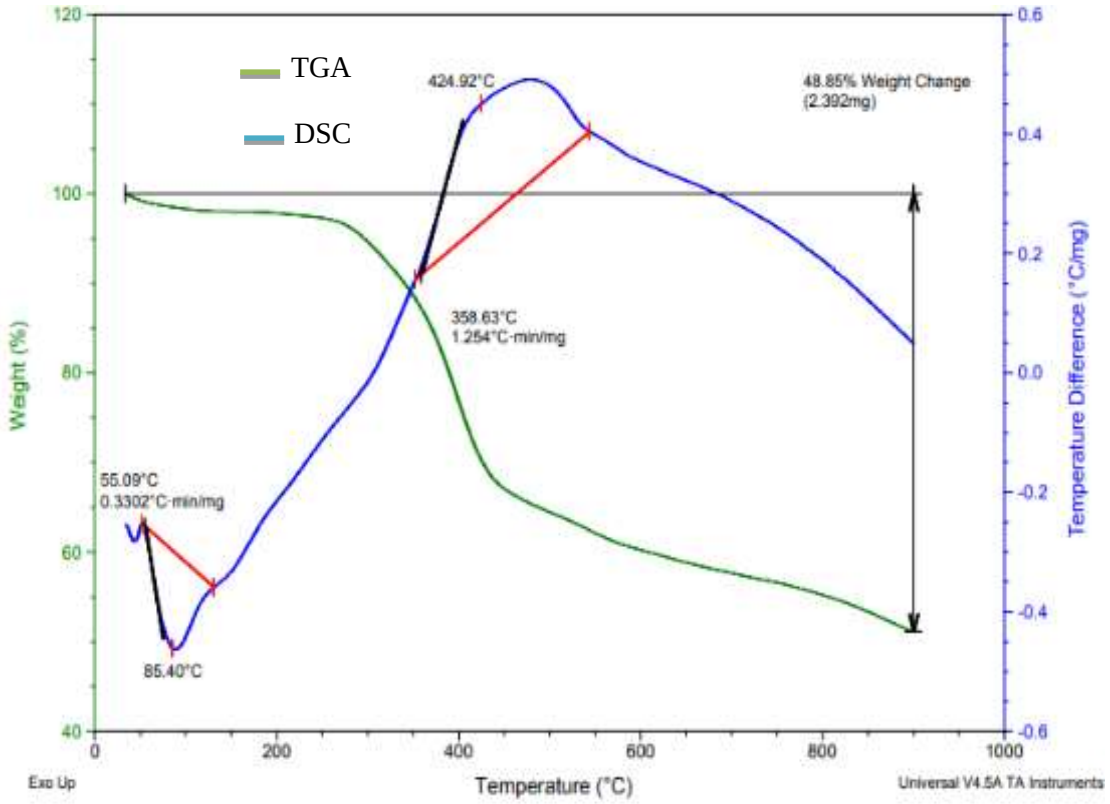

Figure 3.2: TGA/DSC of RHAPSA@Dir.

3.1.4 X-ray Diffraction (XRD)

X-ray Diffraction is a crucial method for characterizing materials and determining whether they are crystalline or amorphous. By making estimates, this method sheds light on the sample's composition and calculates the scattering angles and strength with Bragg's equation.

$n\lambda = 2d \sin \theta$

An XRD analysis of RHAPSA@Dir showed the presence of a wide diffused band, with maximal 2θ at 22.8°. This finding corroborates the amorphous character of the functionalized silica analyzed and agrees with the strong broad band of amorphous silica as in Fig. 3.3 [98].

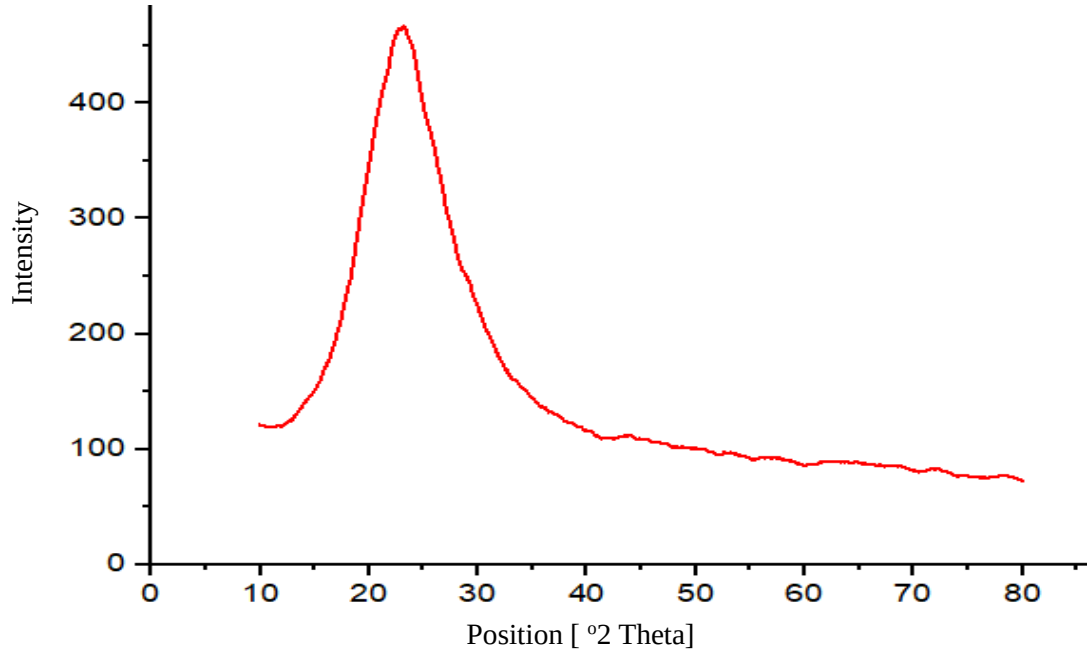

Figure 3.3: The XRD of RHAPSA@Dir.

3.1.5 Nitrogen adsorption –desorption

Fig. 3.4 displays the nitrogen adsorption isotherm for RHAPSA@Dir. Fig. 3.5 shows a graph depicting the pore size distribution. Capillary condensation, as classified by the IUPAC, is connected to the hysteresis loop that may be seen between the values of 0.4 and 1.0. The isotherm had a type IV shape and an H3 hysteresis loop[99]. RHAPSA@Dir was found to have a specific surface area of approximately 416.3 m^2gm^{-1} and an average pore volume of 0.26 cm^3/gm. After the immobilization of pyridine sulfonic acid on silica the specific surface area was reduced-by RHACCl (633 m^2 gm^{-1}) [92] .Because the surface was overcrowded with pyridine sulfonic acid it closed the pores which reducing in the surface area. The

microspores of SiO_2 have an average pore diameter of 10.4 nm (Table 3.2), RHACCl had an average pore diameter of 6.07 nm, and RHAPSA@Dir showed 3.1 nm. This result was showed RHAPSA@Dir has the smallest pore volume compared to both RHA and RHACCl.

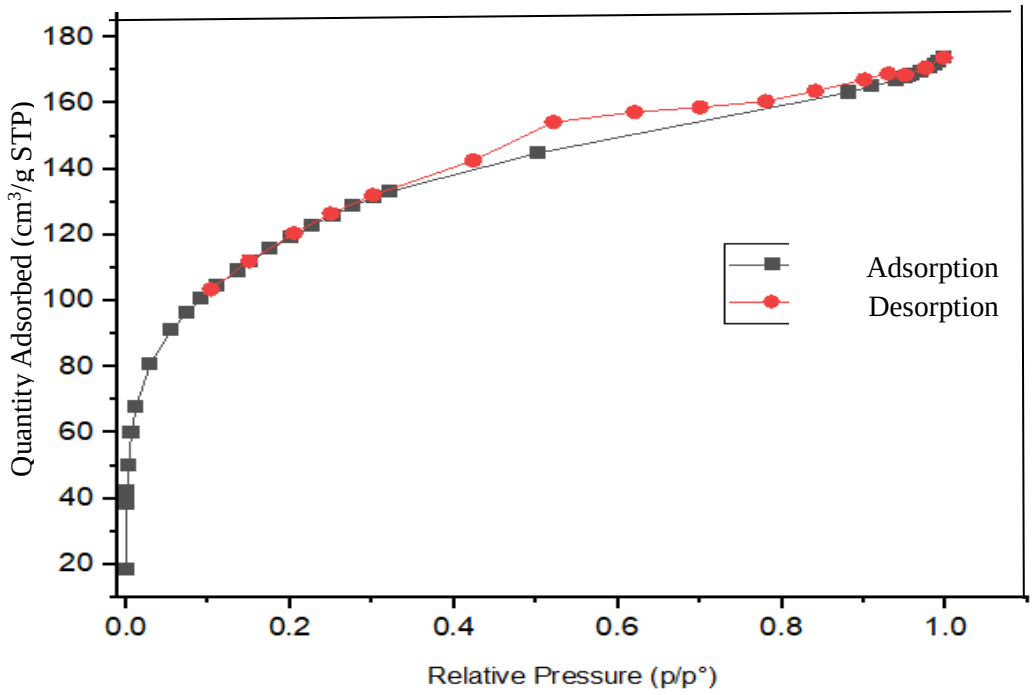

Figure 3.4: The N_2 adsorption-desorption isotherms of RHAPSA@Dir.

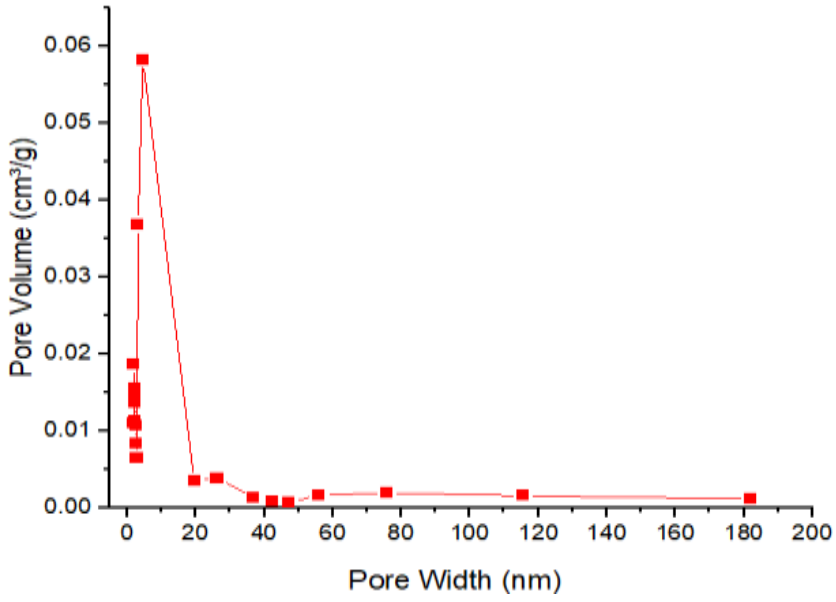

Figure 3.5: Graph showing the distribution of pore sizes of of RHAPSA@Dir.

Table 3.2: The specific surface area, Average pore volume, and average pore diameter of RHA, RHACCl, and RHAPSA@Dir.

Sample	Specific surface area (m^2g^{-1})	Average pore volume (cc g^{-1})	Average pore diameter(nm)
RHA [91]	347	0.87	10.4
RHACCl [92]	633	0.70	6.07
RHAPSA@Dir	416	0.26	3.1

3.1.6 Scanning electron microscopy

SEM images of RHAPSA@Dir were given in Fig.3.6(a, b, and c). The analyses confirmed that the surface was rough, and a slight degree of pores arrangement was seen. Shapes were seen with a few micrometres in length and a few nanometres in width (Fig. 3.6 (a). No more specific shapes were seen.

3.1.7 Transition electron microscopy

The TEM micrograph of RHAPSA@Dir is given in Fig.3.7 (a, b). Spherical nanoparticles were deducted. Each spherical particle had an approximation diameter of 6 nm. The particles were distributed randomly.

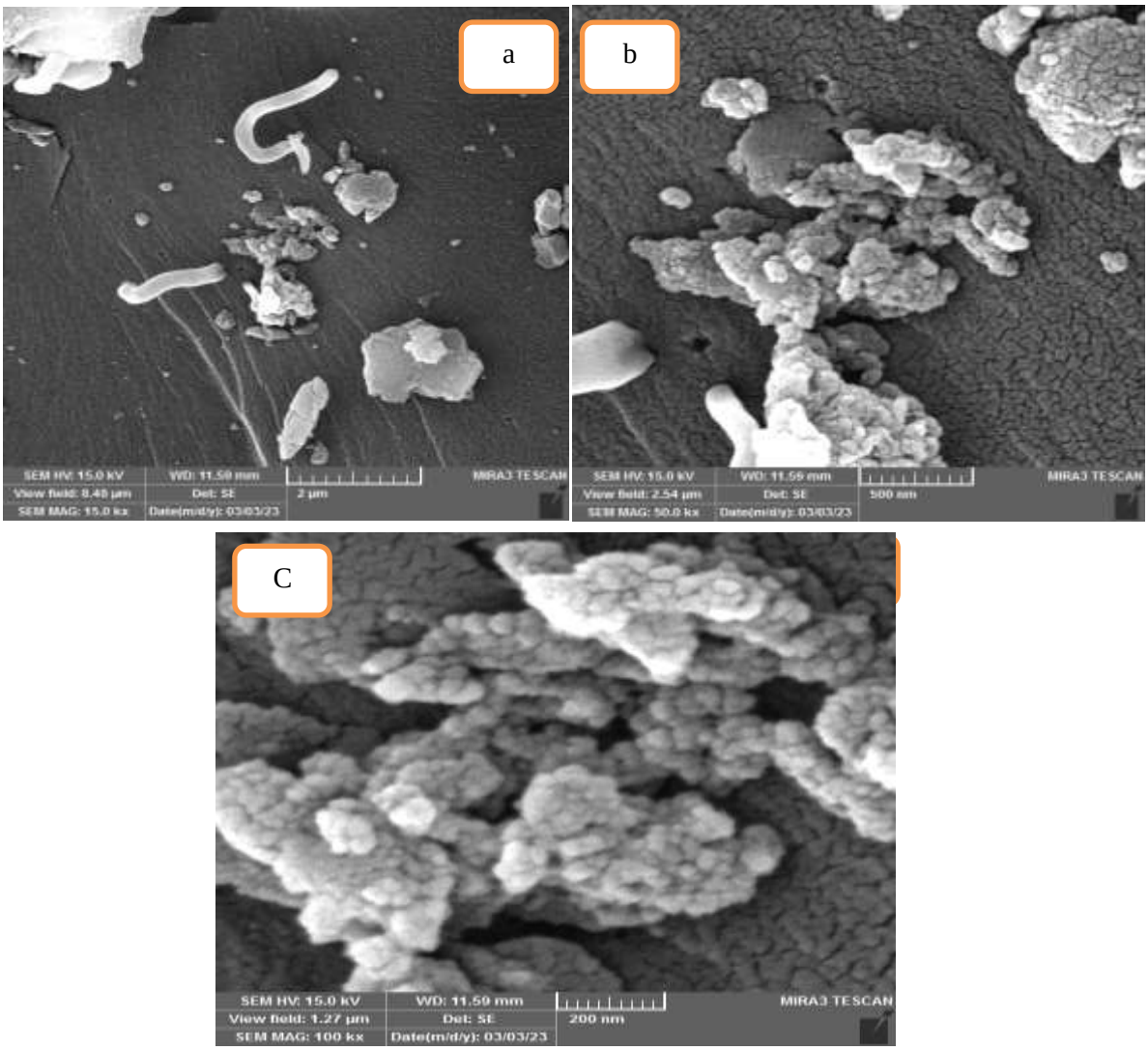

Figure 3.6: The SEM micrographs of the RHAPSA@Dir (a) 2 um, (b)500 nm,(c) 200 nm**.**

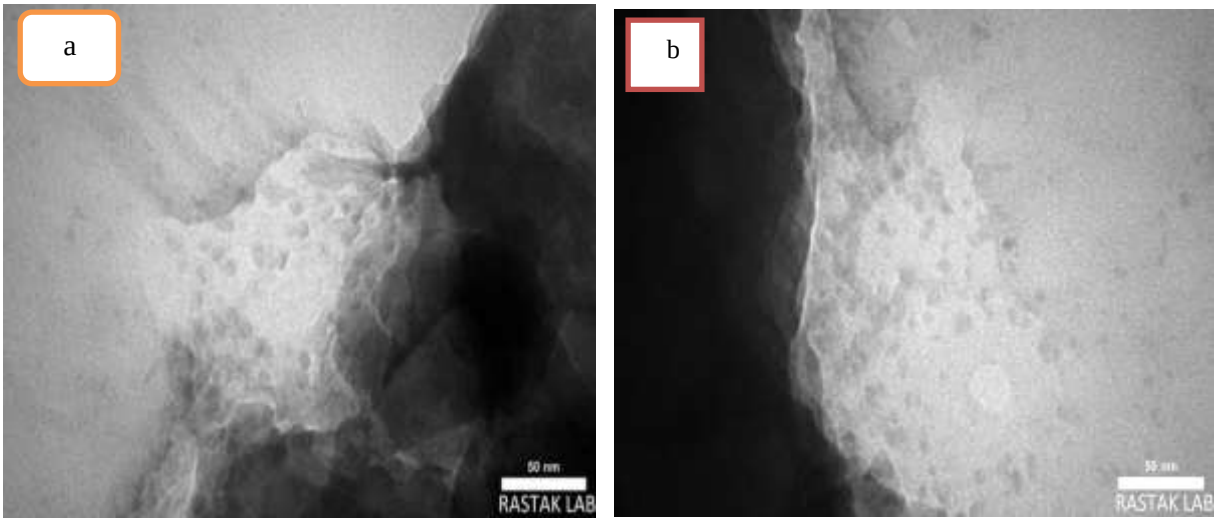

Figure 3.7: The TEM micrographs of the RHAPSA@Dir (a)50nm,(b)50nm.

3.2 Immobilizing of pyridine sulfonic acid onto silica by post modification method

CPTES was added to sodium silicate in the direct homogenous method the (Sol-Gel technique). The resultant product was then used in the post-synthesis procedure to produce the catalyst which was labeled as RHAPSA@Ref. A nucleophilic substitution of chlorine in silica -CH_2 Cl by pyridine sulfonic acid was taking place as in Scheme 3.2.

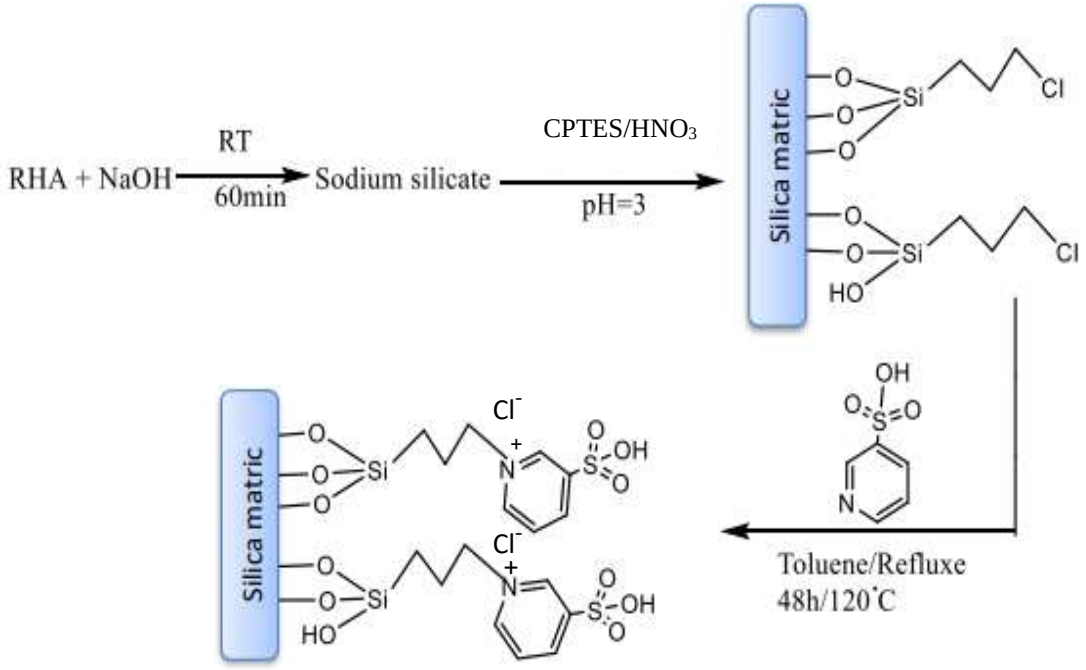

Scheme 3.2: RHAPSA@Ref catalyst synthesis process.

3.2.1 FT-IR spectral analysis

RHAPSA@Ref and RHA and RHACCl FT-IR spectrum were shown in Figure 3.8. At 1090 cm^{-1} in the RHA spectrum Si-O-Si vibrations were observed. For RHAPSA@Ref the Si-O-Si vibrations were seen at 1076 cm^{-1} .O-H vibrations were observed in the range of 3457-3443 cm^{-1} [95]. The band at 3090 cm^{-1} indicates the presence of C-H aromatic which was related to the pyridine ring. At a frequency of 2940 cm^{-1}, the C-H aliphatic was observed. The band at a frequency of 1230 cm^{-1}corresponded to the Si-C bond. The -CH_2- group was showing at a frequency of

1443 cm^{-1}. RHAPSA@Ref spectra exhibit a band between 1370 and 1193 cm^{-1} due to SO_2 stretching bands. At 3090 cm^{-1}, RHAPSA@Ref detects the aromatic C-H stretching vibration. All these absorption bands inducted to the successful laded of silica with pyridine sulfonic acid [96].

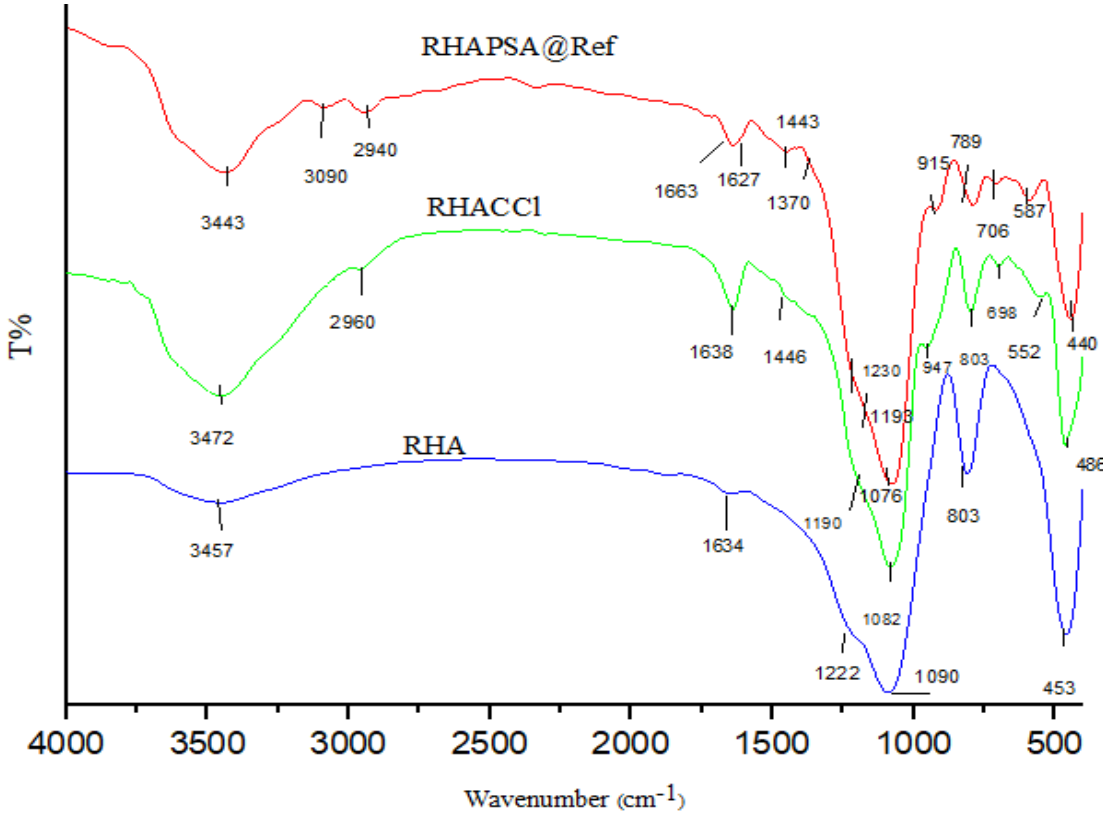

Figure 3.8: The FT-IR spectra of RHAPSA@Ref and RHA and RHACCl.

3.2.2 Elemental analysis (C.H.N.S)

Elemental data for RHA, RHACCl, and RHAPSA@Ref were shown in Table 3.3. The percentage of carbon in RHA was 0.42 % and 1.76 % in hydrogen [83]. RHACCl had 11.9 % of carbon and 1.91% hydrogen. RHAPSA@ Ref showed 14.94 % of carbon and 2.15 % sulfur and 1.11 % of Nitrogen. The presence of Sulfur and Nitrogen with the increased Carbon percentage indicated that PSA was incorporated into the silica structure. It was observed that RHAPSA@Ref had a percentage of C, S, and N higher than RHAPSA@Dir.

Table 3.3: Elemental analysis data of RHA, RHACCl, and RHAPSA@Ref.

Sample	**Elemental analysis %**			
	C	H	N	S
RHA[83]	0.42	1.76	_	_
RHACCl[92]	11.90	1.90	_	_
RHAPSA@Ref	14.94	2.02	1.11	2.15

3.2.3 Nitrogen adsorption –desorption

The nitrogen adsorption isotherm of RHAPSA@Ref is show in Fig. 3.9. Figure 3.10 displayed the graph of pore size distribution. Even when relative pressure reached zero, the RHAPSA@ Ref hysteresis loop was not closed. This is not an ordinary hysteresis loop the pore like ink-buttle shape. A similar finding was observed with another ligand that had sulphonic groups on silica [83] .Pore size distribution was observed in the range of 1-15 nm and another pore in the range of 17-36 nm. These results indicated that RHAPSA@ Ref had two types of pore fall in the micropores and mesoporous range.

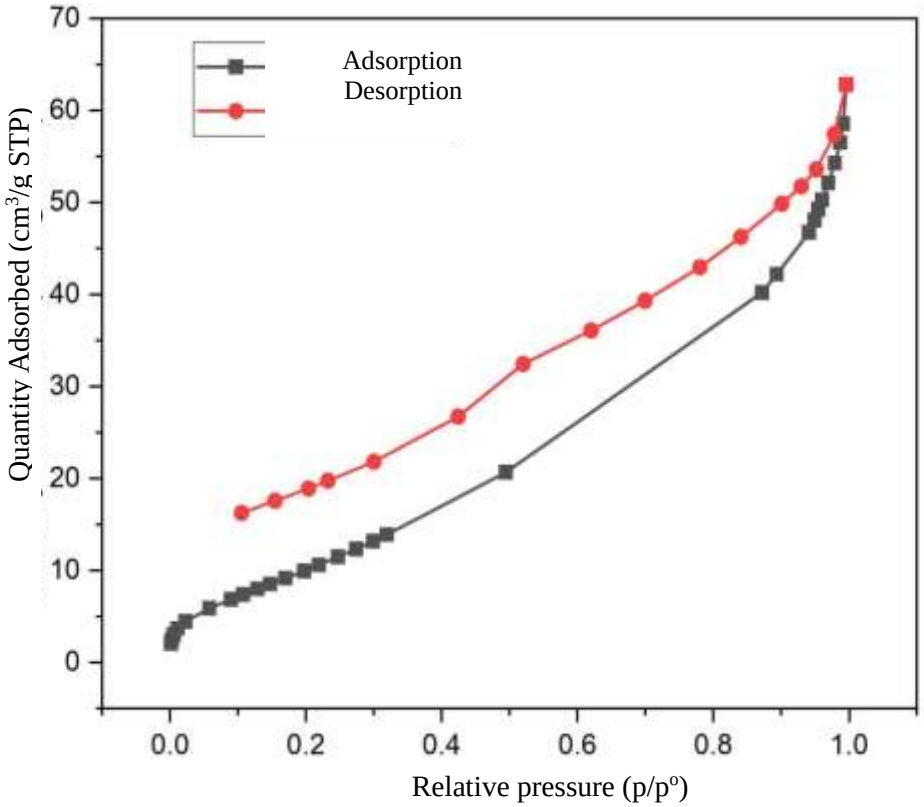

Figure 3.9: The N_2 adsorption – desorption isotherms of RHAPSA@Ref.

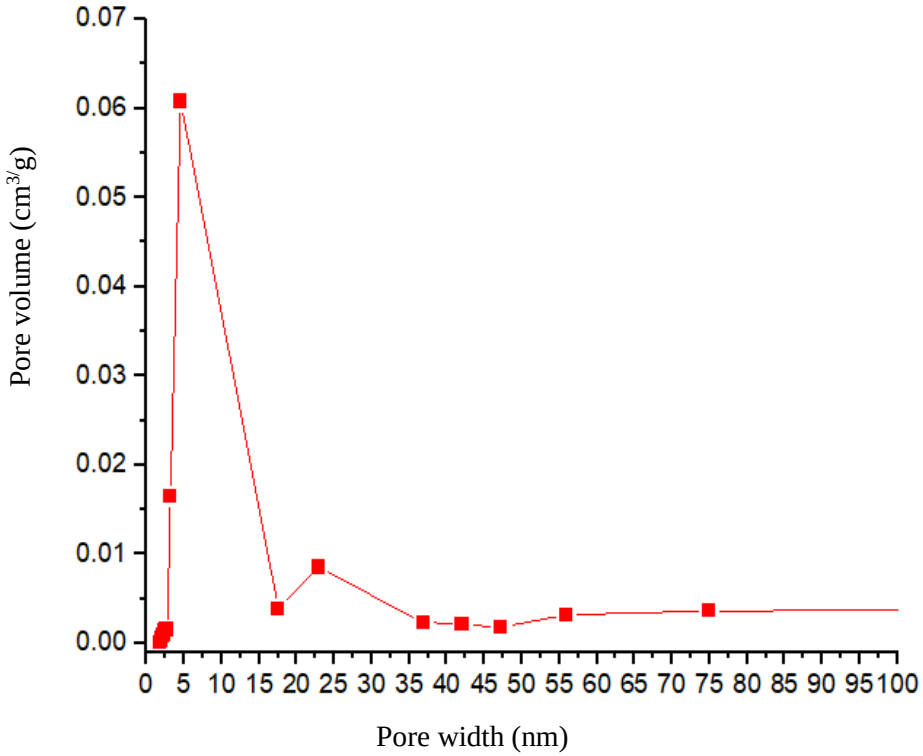

Figure 3.10: The graph is showing the of pore sizes distribution of RHAPSA@Ref.

3.2.4 TGA/DSC of RHAPSA@Ref.

Fig.3.11 displays the results of the thermogravimetric graph of RHAPSA@Ref. Three different decomposition stages were seen in the TGA/DSC graph. The first mass loss of about 4 % was observed in the range of 36-140 ^{o}C due to the loss of physically absorbed water. About 30 % of mass loss was observed in the range of 250-400 ^{o}C related to the decomposition of organic loaded onto silica (pyridine sulfonic acid and CPTES). The mass losses between 600 and 900 ˚C (15%) were thought to be due to the silanol aggregates [97]. The DSC curve shows two exothermic and endothermic transitions, the first peak of which occurs between 138 and 180 °C with a maximum of 156.69 °C as a result of losing absorbed water. The second mass loss happens between 372 and 527 °C, with a peak centred at 432.41 °C. The second transformation was referring to the organic material removed from the catalyst. The third phase happens between 527 and 900 °C as a result of silanol condensation[90].

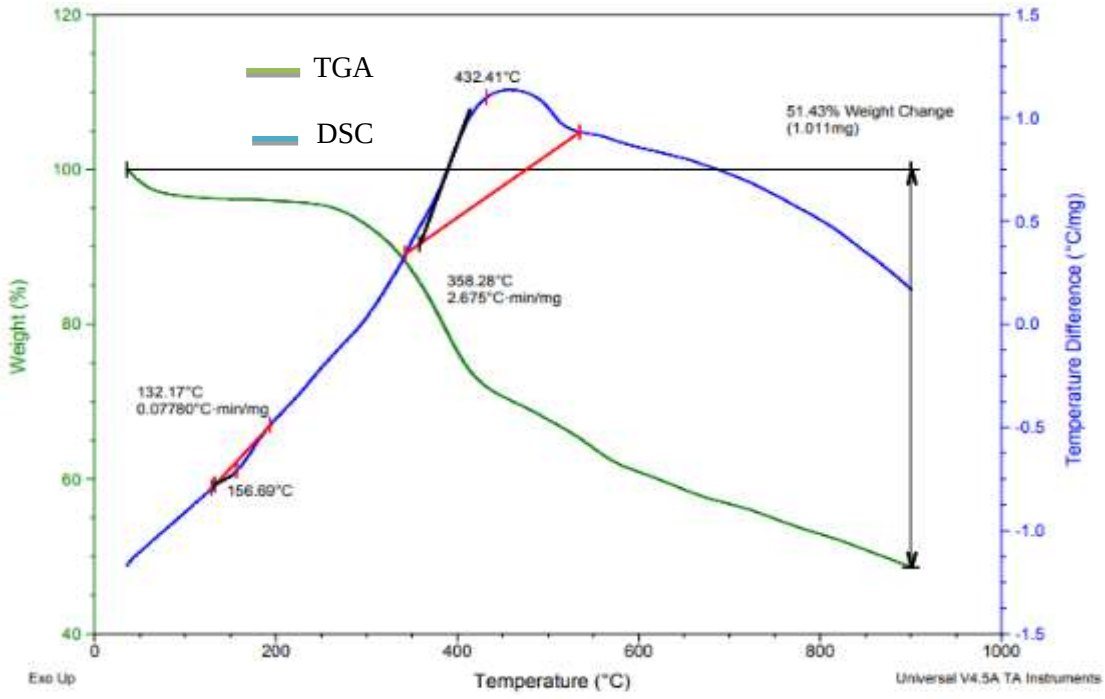

Figure3.11: TGA and DSC of RHAPSA@Ref.

3.2.5 X-ray Diffraction (XRD)

Fig. 3.12 shows the X-ray powder diffraction pattern for RHAPSA@Ref.It appears that the samples are amorphous because that only broad pattern at a 2 θ angle of around 23^{o} was observed.

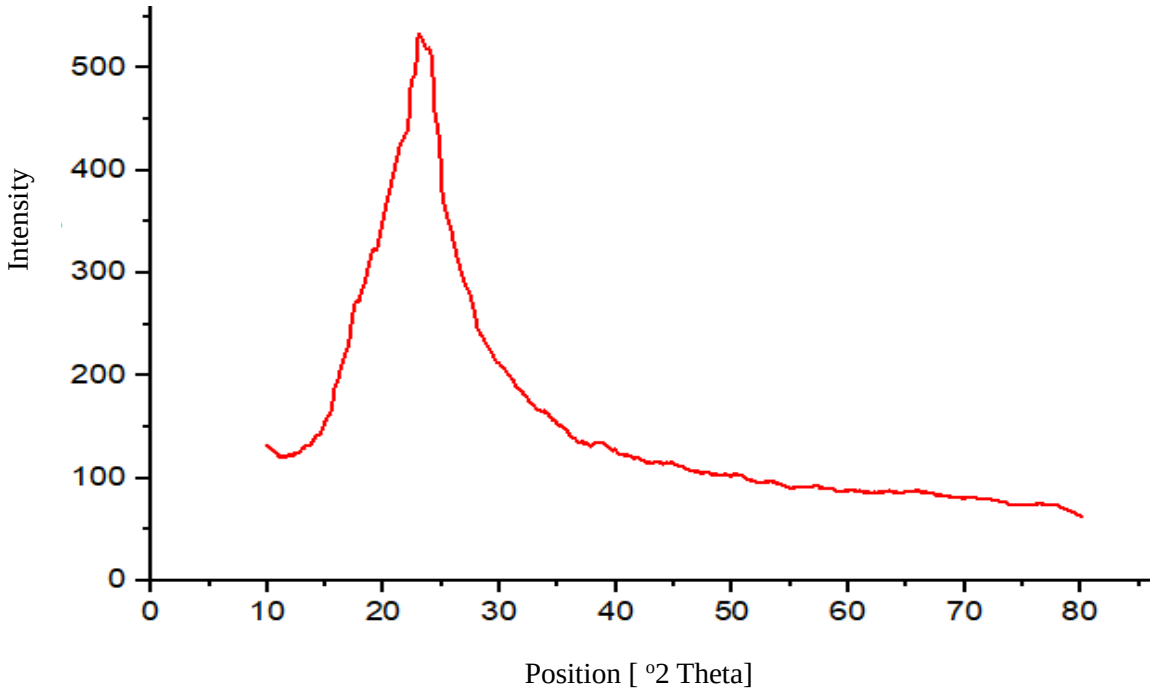

Figure 3.12: The XRD of RHAPSA@Ref.

3.2.6 Electron Microscopy (TEM and SEM)

Scanning electron microscopy of RHAPSA@Ref is given in Figure 13(a, b, and c). The rough porous surface with large particles was seen. Even those large particles were porous too. The TEM micrograph Fig.14(a, b) of RHAPSA@Ref is given. The sample had aggregate particles. No specific shape was found. The figure 3-14 (b) showed some geometrical particles were closed to each other's.

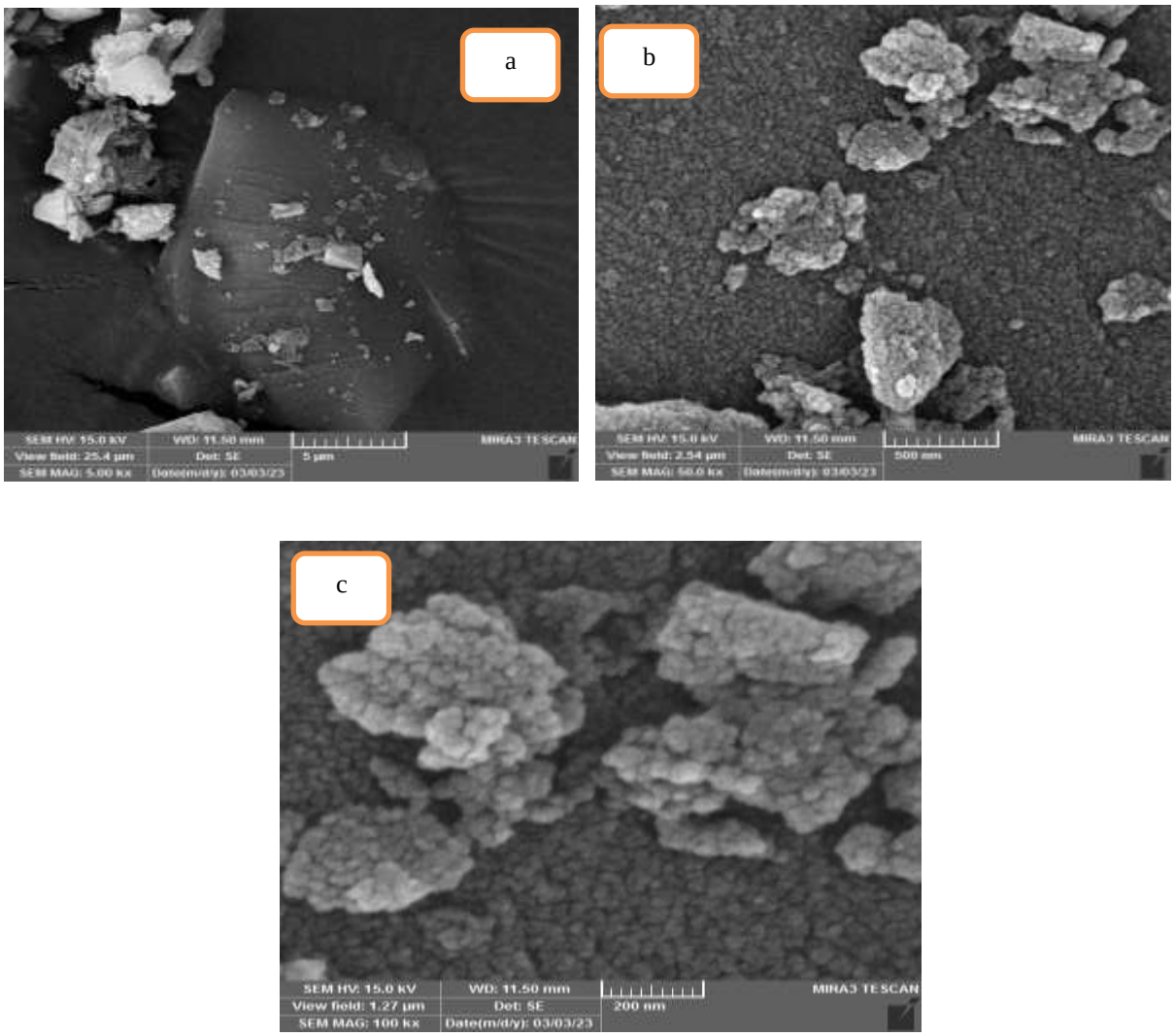

Figure .3.13: The SEM micrographs of the RHAPSA@Ref (a)5um,(b)500nm,(c)200nm.

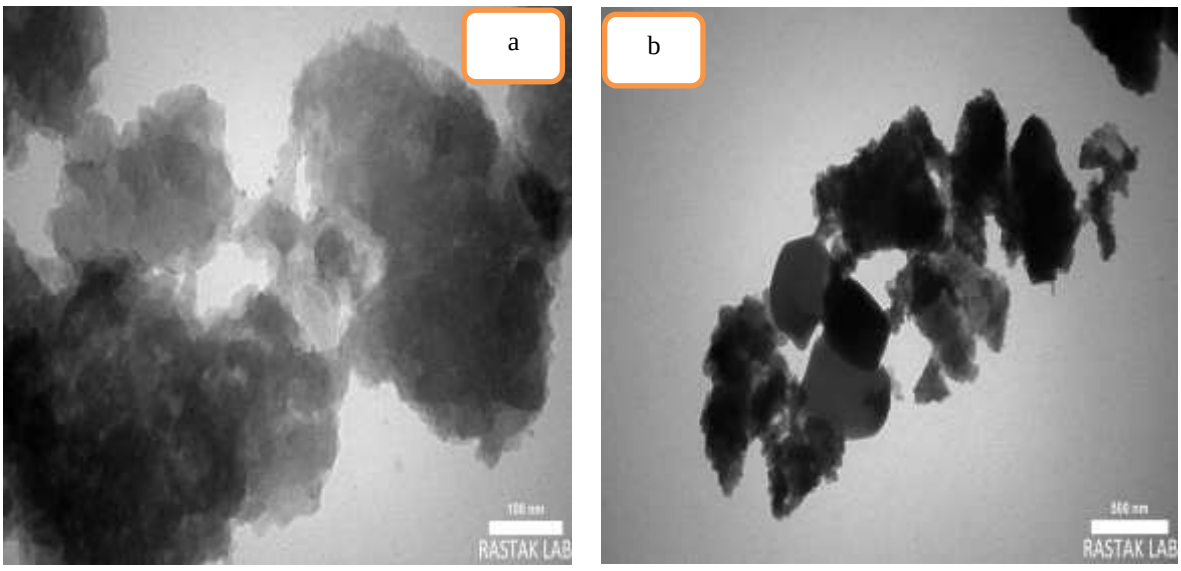

Figure .3.14: The TEM micrographs of the RHAPSA@Ref (a)100 nm,(b) 500 nm.

3.3 Determination of glucose concentration

The visual methods are used to determine the glucose concentration changes. 3,5-dinitrosalicylic acid (DNS) technique [94] was used for this purpose by converting DNS to its reduced form 3-amino-5-nitrosalicylic acid, via oxidizes the aldehyde group of glucose Scheme 3-3. 3-Amino-5-nitrosalicylic acid is produced in a linear structure as a function of glucose concentration. The amount of light absorbed at 540 nm was measured due to the production of 3-amino-5-nitrosalicylic acid.

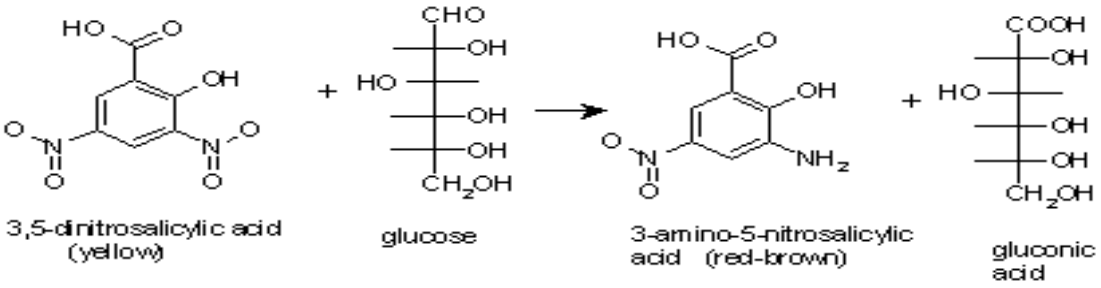

Scheme 3.3. Glucose reduction by DNS reagent [100].

3.4 Cellulose hydrolysis and Glucose degradation over pyridine sulfonic acid

Cellulose and glucose were hydrolyses using a homogenous catalyst pyridine sulfonic acid in simple procedures and conditions. Various variables have been evaluated to improve hydrolysis conditions, such as time, mass, temperature, and solvents below are the details of the parameters evaluated over the pyridine sulfonic acid homogenous catalyst.

3.4.1 Time protocol

Fig. 3-15 depicts the influence of time hydrolysis over pyridine sulfonic acid. At 130 ℃, 0.1 gm of pyridine sulfonic acid and 0.1gm of glucose and cellulose were

dissolved in a DMF\LiCl(25mL/0.5gm) mixture to perform the hydrolysis. Cellulose hydrolysis was started after the reaction took place and reached to 98% after 6 hours. However, the percentage of glucose produced during in-situ hydrolysis of glucose into other products was found to decrease with increasing hydrolysis time (greater than 6 hours). In a separate experiment, glucose was tested for hydrolysis over the pyridine sulfonic acid catalyst. The results showed that the glucose was fully degraded within 3 h into other products. No more change in the degradation of glucose was observed after 4 hours of the reaction. Therefore, the optimal hydrolysis times for cellulose to glucose and glucose to other products over pyridine sulfonic acid were six and three hours, respectively.

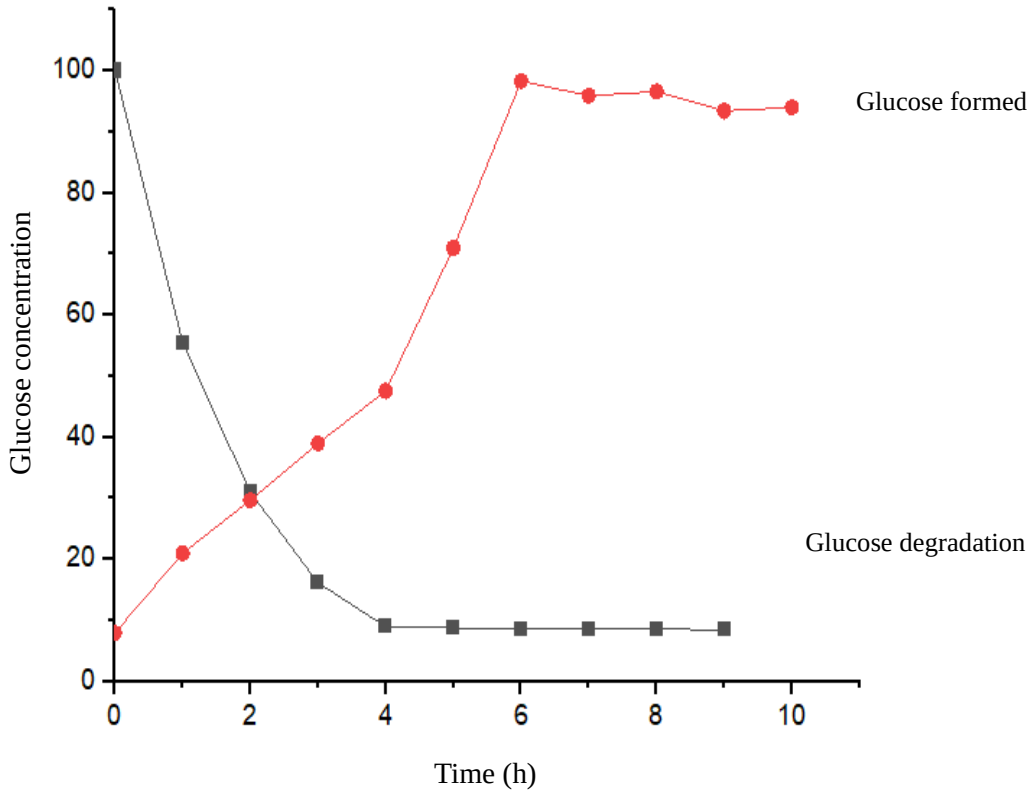

Figure 3.15: Glucose formed from cellulose hydrolysis and glucose degradation over pyridine sulfonic acid as a function to the time. The hydrolysis condition was 0.1 gm mass of catalyst, at 130 °C.

3.4.2 Mass effect

Hydrolysis of cellulose and glucose is performed by adjusting the concentration of pyridine sulfonic acid (in the range of 0.05, 0.1, and 0.15 gm) while holding all other parameters constant (hydrolysis time of 10 hours, and 130 °C temperature) (Fig.3-16). Cellulose hydrolysis increased clearly from 45% to 98% with a rise from 0.05 to 0.15 gm of catalyst mass. Glucose was degradation very fast over both 0.1 and 0.15 gm of the catalyst mass. 0.05 gm has good results too for both hydrolysis; however, the hydrolysis seems to be slower compared with other masses. The best hydrolysis results were obtained during the use of 0.1 gm as a catalyst mass.

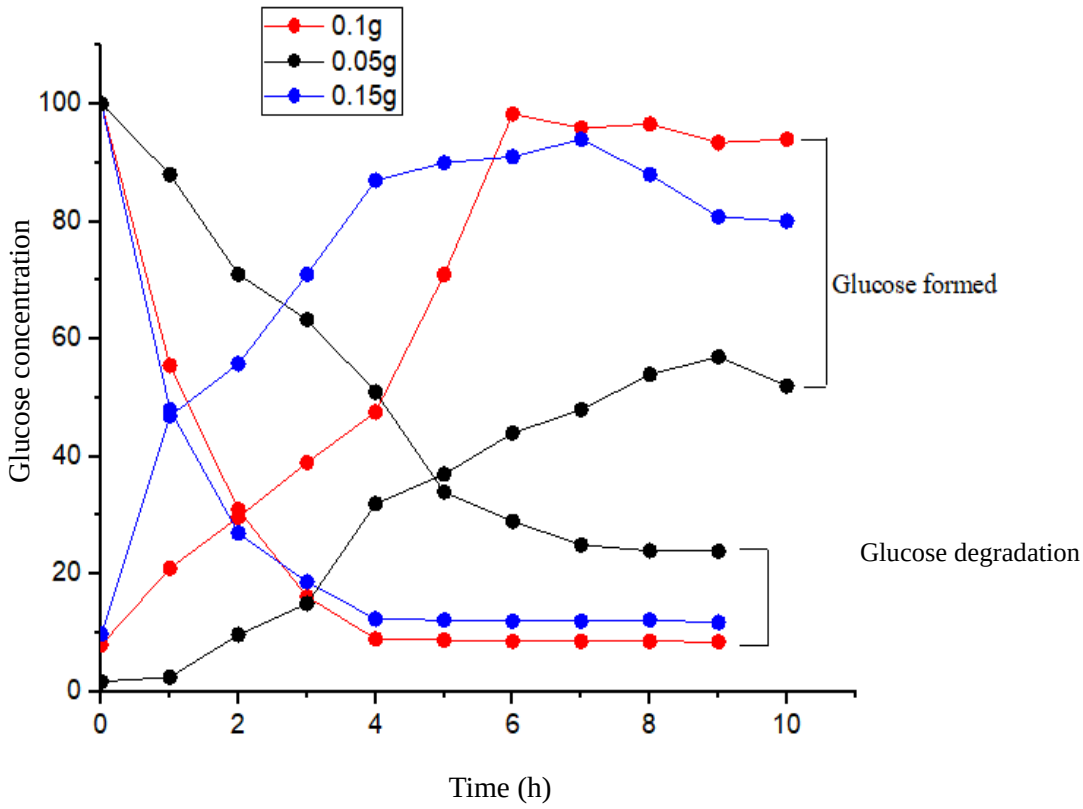

Figure 3-16: The hydrolysis of cellulose and glucose degradation over pyridine sulfonic acid as function to catalyst mass.

3.4.3 Hydrolysis temperature

Fig.3-17 showed the results of using three different temperatures for the hydrolysis of cellulose and glucose degradation. On the cellulose hydrolysis profile, the glucose formed was 49 % at 110 °C during the six hours. This percentage was increased to 98 % at 130 °C at the same time. On the glucose degradation profile, the glucose degradation was 40 % at 110 °C during the 4 hours. This percentage was increased to 90 % at 130 °C during the second hour. It was choosing 130 °C as the optimum temperature for both hydrolyses as a result of good hydrolysis observed.

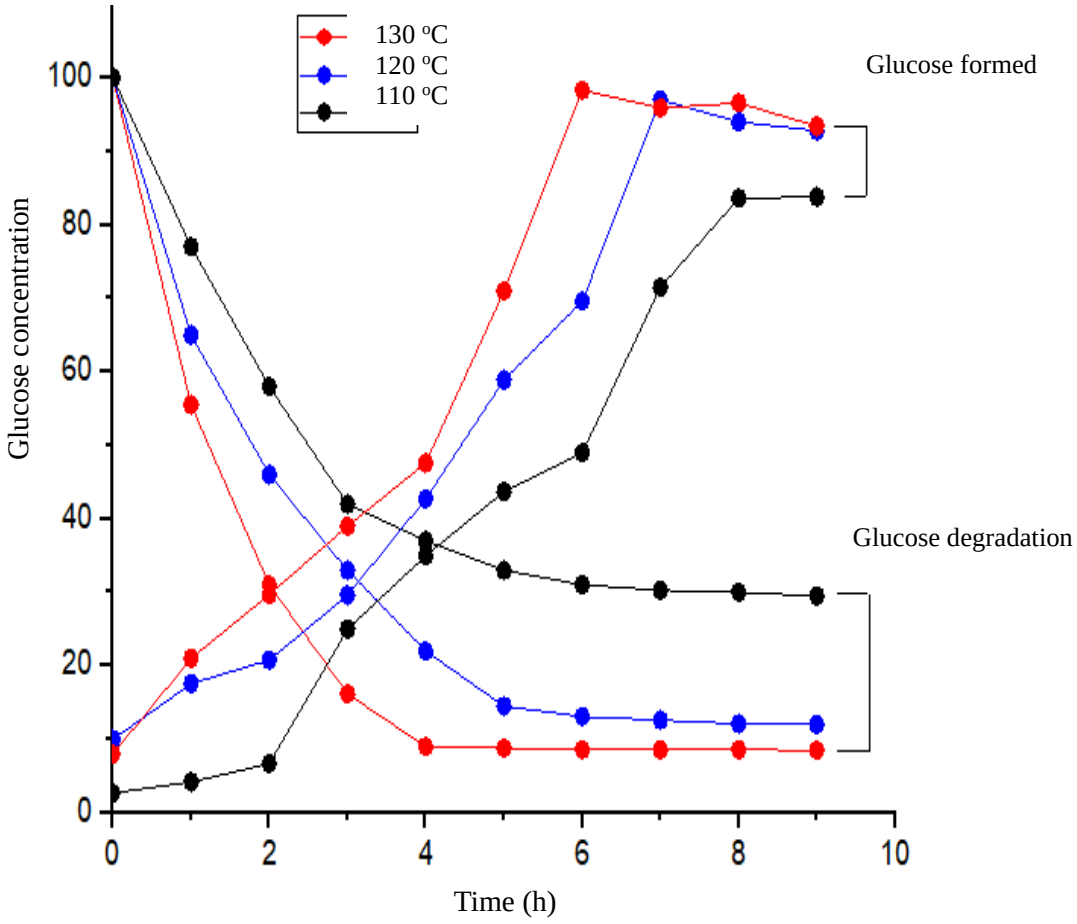

Figure 3.17: Cellulose hydrolysis and glucose degradation over pyridine sulfonic acid at different temperatures.

3.4.4 Solvents effect

Different solvents were used for testing the cellulose hydrolysis and glucose degradation. This solvent was included DMF, cyclohexanol, toluene, and 1-butanol as in Fig. 3-18. Each hydrolysis was found to have flowed the following pattern.

DMF > cyclohexanol >1-butanol> toluene

The ability of the solvent to dissolve cellulose was an essential point of the hydrolysis process. The DMF including LiCl had the best ability to dissolve cellulose. Cyclohexanol and 1-butanol also showed good results compared with other solvents. Similar behavior for solvents deducted during the glucose hydrolysis. Toluene in each hydrolysis and degradation were not giving good results. The hydrogen bonds could be formed in all solvents with the starting material. Toluene was not able to form hydrogen bonding with the starting material which led to decreased hydrolysis rate.

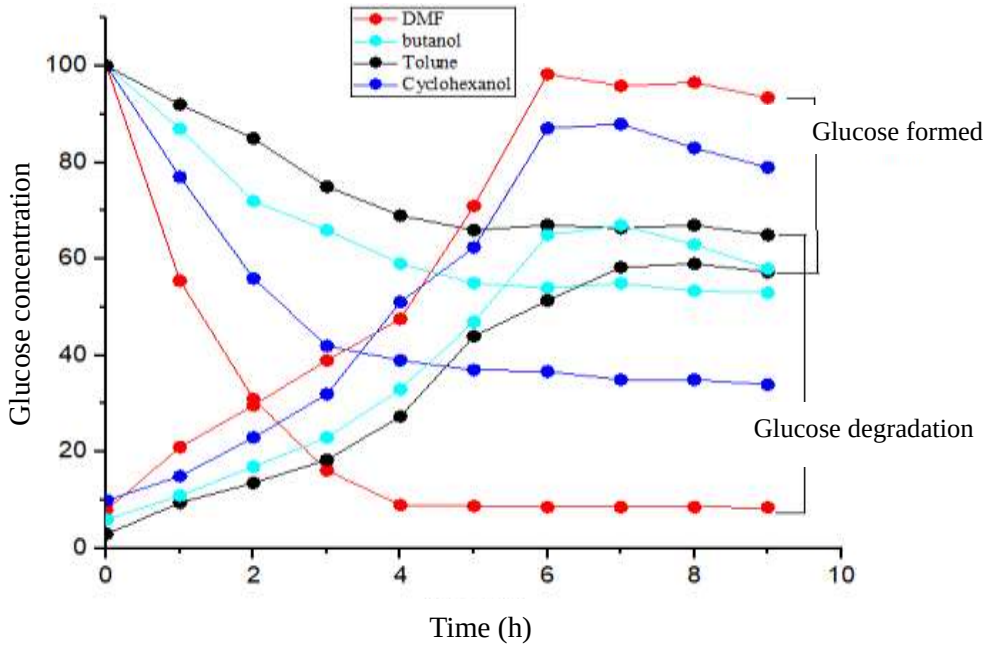

Figure 3-18: Cellulose hydrolysis and glucose degradation over pyridine sulfonic acid at different solvents.

3.5 Cellulose hydrolysis and glucose degradation over RHAPSA@Dir

Cellulose and glucose were used for hydrolysis to other products over the RHAPSA@Dir. Hydrolysis conditions were optimized by investigating the effects of mass, temperature, solvents, and other parameters on the final product. When conducting the hydrolysis of cellulose to glucose and measuring the concentration of the glucose decomposed, it was noticing low rates of up to 8 hours. It contains 55 percent of glucose. The low concentration of formed glucose could be due to the fact that glucose able to hydrolysis. To prove that a separate experiment, used glucose for degradation over the RHAPSA@Dir to form other compounds has done. It was noticed that after 6 hours, the percentage of glucose was decreased from 100 to 14 %. This resat clearly indicated the activity of the catalyst for both cellulose hydrolysis and glucose degradation as shown in fig. 3-19.

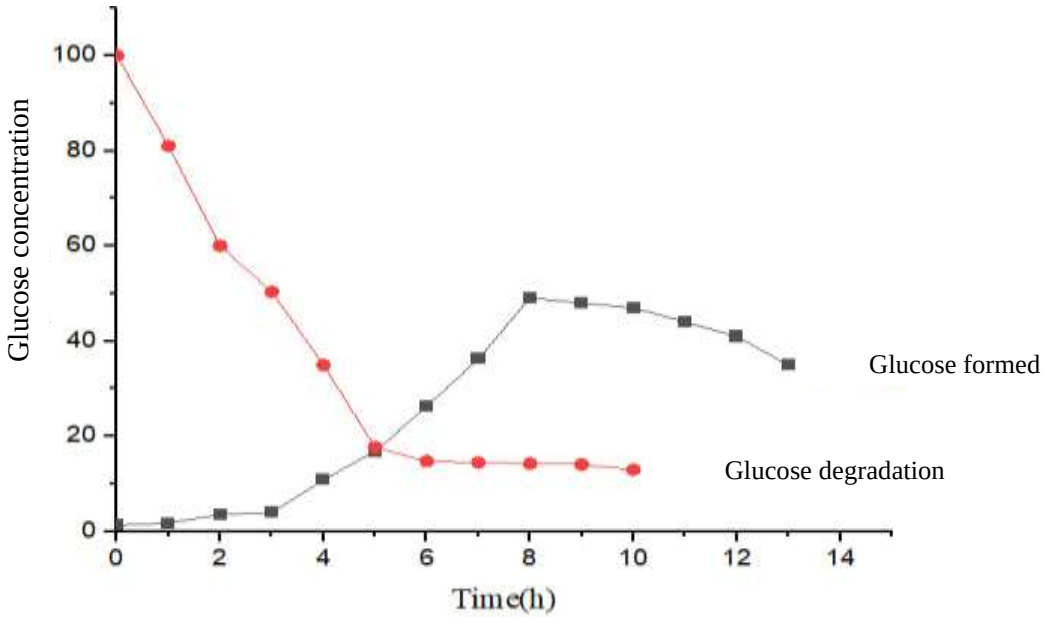

Figure.3.19: Hydrolysis cellulose and glucose degradation over RHAPSA@Dir at 140^{o}C as a function of time.

3.5.1 Mass effect

Fig.3.20 showed that 0.1 gm was the best mass used among three different masses used for cellulose hydrolysis, while 0.15 gm was the best mass may use for glucose degradation. All masses were run at 140 °C for 10 hours in glucose degradation and 13 hours for hydrolysis cellulose.

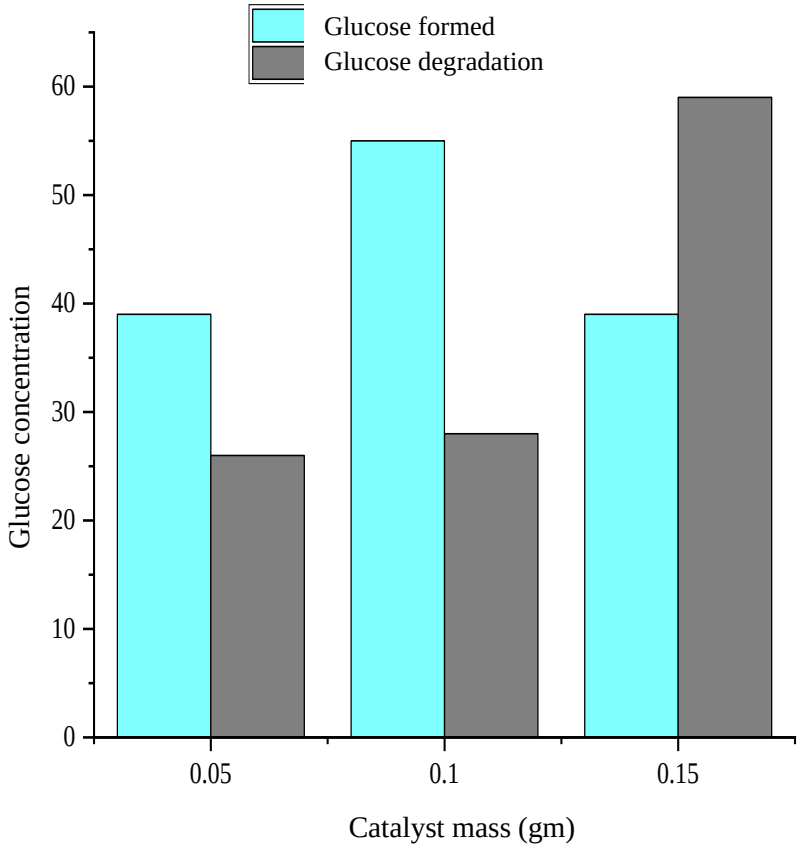

Figure3.20: Cellulose hydrolysis and glucose degradation over RHAPSA@Dir at140^{o}C as a function for catalyst mass.

3.5.2 Hydrolysis temperature

Three different temperatures120, 130, and 140 °C were applied to the degradation of glucose and cellulose hydrolysis over RHAPSA@Dir as in Fig. 3.21. In general, hydrolysis increased when the temperature was increased over the catalyst. 140 °C was selected as the best temperature for both hydrolyses and degradation over the RHAPSA@Dir.

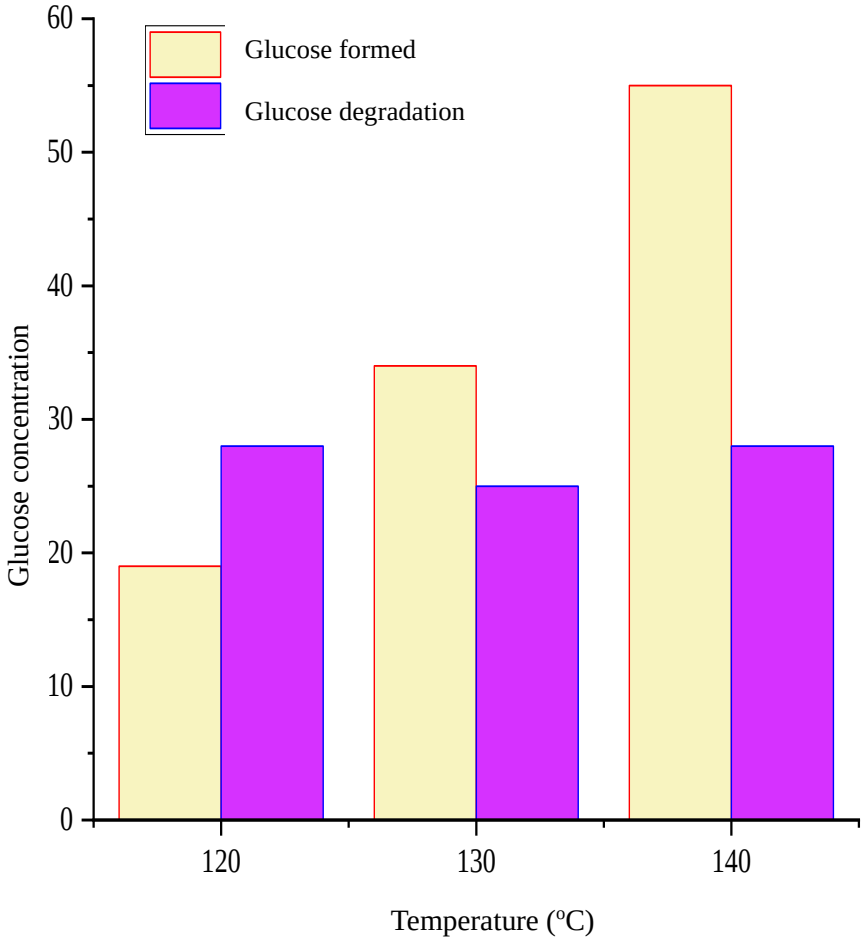

Figure 3.21: Effect of different temperature on the cellulose hydrolysis e and glucose degradation over RHAPSA@Dir.

3.5.3 Solvents effect

In Fig. 3-22, the effect of 1-butanol, dimethylformamide, and cyclohexanol on the degradation of glucose and cellulose hydrolysis is shown. DMF showed that cellulose hydrolysis can easily and 1-Butanol glucose degradation can easily. While Cyclohexanol was the worst solvent for degradation glucose and hydrolysis cellulose.

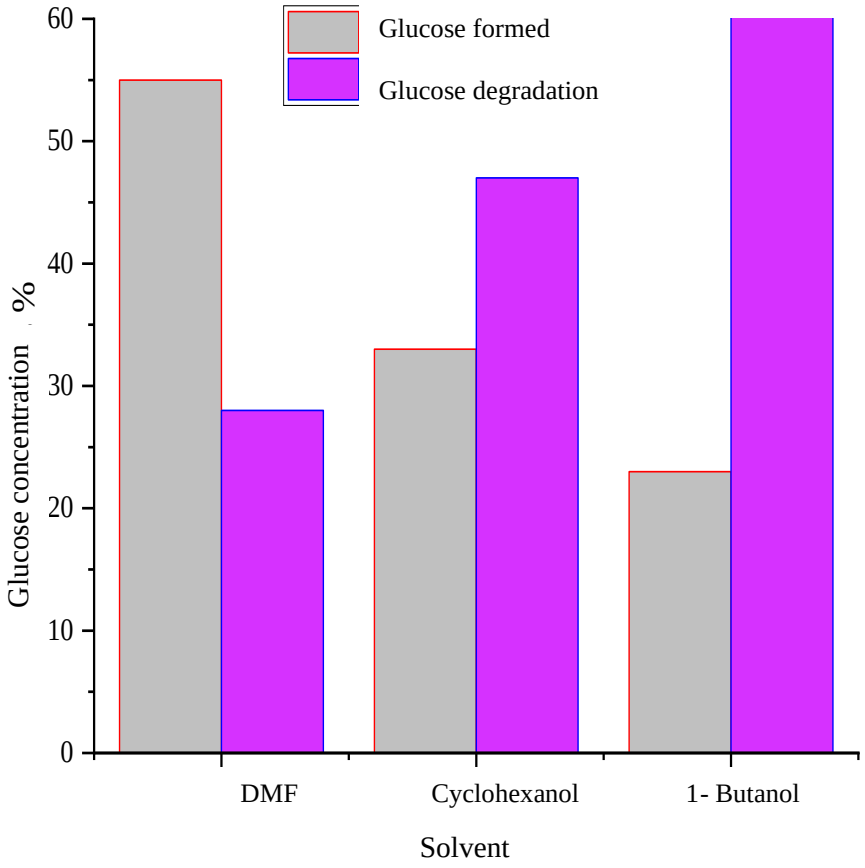

Figure 3.22: degradation glucose and cellulose hydrolysis over heterogeneous RHAPSA@dir and 140^{o}C at different solvent.

3.6 Catalyst regeneration experiments

The catalyst was reactivated at 110 °C for 24 hours after being rinsed twice with hot DMF following the initial hydrolysis with RHAPSA@Dir. After that, the identical procedure was repeated for a second round. The same may be said for the third round. It is reasonable to infer that the catalyst retained its effectiveness after being employed. Fig.3.23 displays the obtained data.

.

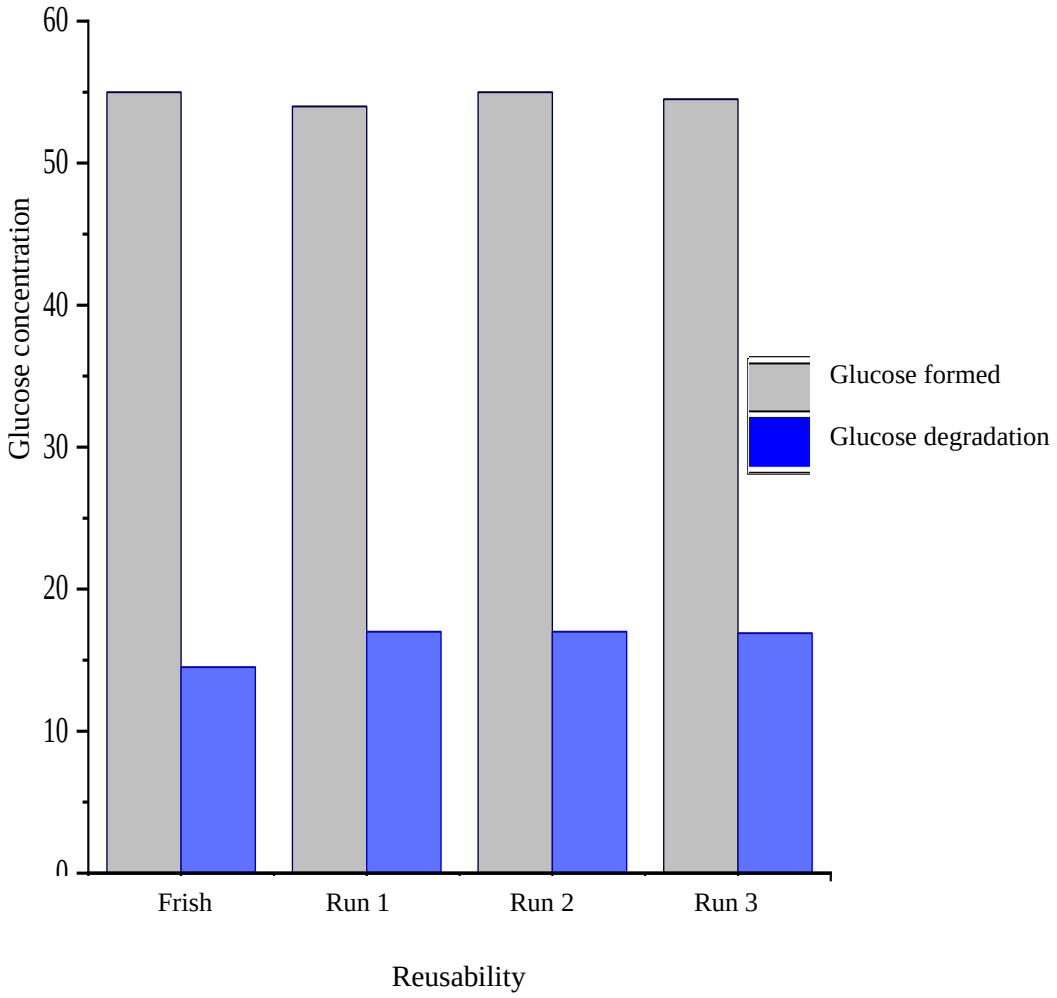

Figure 3.23: Catalyst reusability for the glucose degradation and hydrolysis of cellulose over RHAPSA@Dir.

3.7 Catalytic study over RHAPSA@Dir, RHAPSA@Ref, pyridine sulfonic acid

RHAPSA@Ref and pyridine sulfonic acid and RHAPSA@Dir were run under the optimum conditions. The results were showing in Fig. 3-24. The pyridine sulfonic acid was fully hydrolyzed cellulose and glucose degradation homogenously within 3h for glucose and 6 h for cellulose. The homogenous pyridine sulfonic acid was very active catalyst due to the nature physical of the catalyst as the same phase. RHAPSA@Ref needs 10 h to hydrolysis only 41 % of cellulose, and 4 h to degradation 80 % of glucose, while RHAPSA@Dir needed 9 h to hydrolyze 55 % of

cellulose and 4 h to degradation 86 % of glucose. The activity of RHAPSA@Dir was seeming to be close to the activity of RHAPSA@Ref with short differences in the time of the hydrolysis.

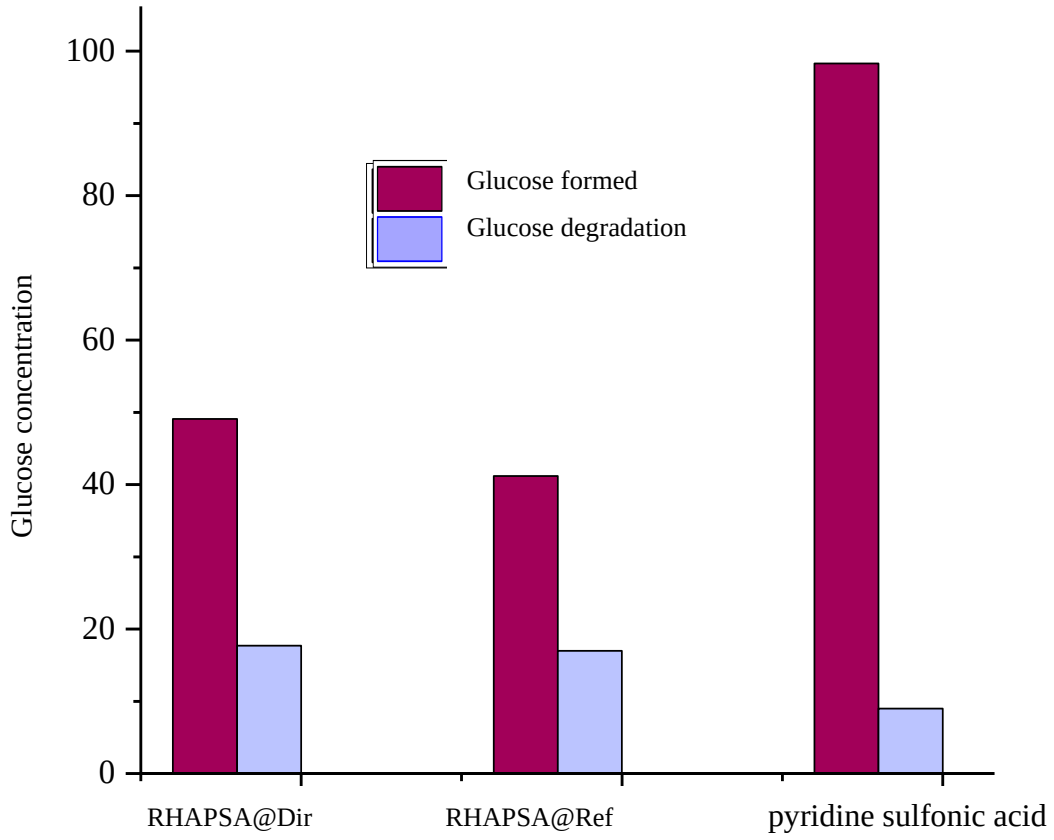

Figure 3.24: Hydrolysis of cellulose to glucose and glucose degradation to other compounds over RHAPSA@Dir, RHAPSA@Ref and pyridine sulfonic acid.

3.8 The physical changes in colour

Fig3.25 shows the physical changes in color after the hydrolysis. After the sample was withdrawn from the mixture, the DNS reagent was added. It was observed that the color was red during the first three hours, then it begins to change to orange at four and five hours and become yellow after six hours. These indicate a decrease in the glucose concentration while also increasing the hydrolysis time.

Figure 3.25: The physical changes in colour of glucose degradation over RHAPSA@Dir.

3.9 GC – Mass investigation

To characterize the products of cellulose hydrolysis, a sample after 10 h of reaction running was injected in GC-Mass. As shown in Fig. 3.26, the main chromatogram showed mullite peaks at different rations. Only CO_2 and H_2O were deducted after matching with GC-Mass library. This result interred that cellulose could fully hydrolysis to CO_2 over the catalyst**.**

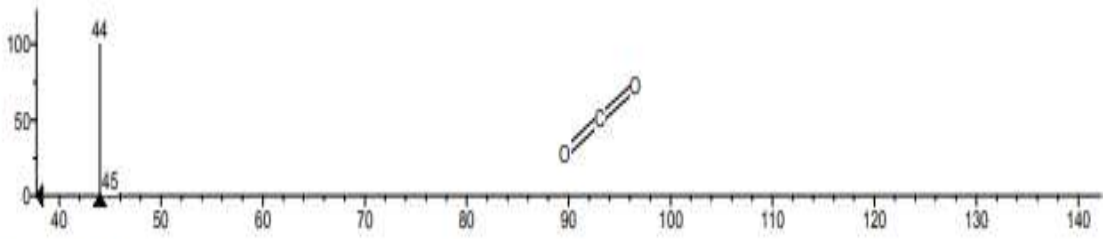

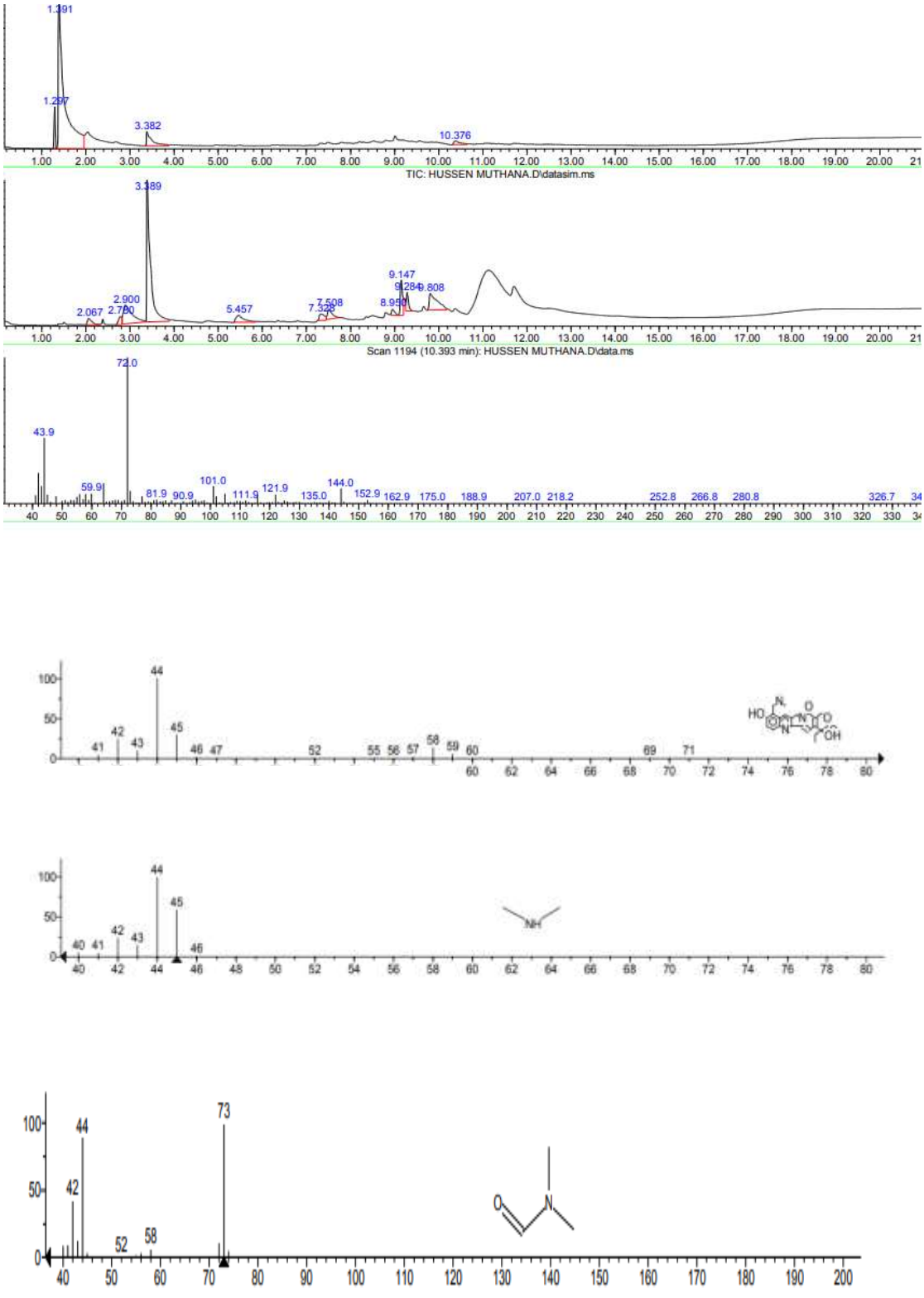

Figure: 3.26. GC – Mass investigation of cellulose hydrolysis over catalyst.

3.10 The suggested hydrolysis mechanism

Cellulose is glucose chain linked by β-glycosidic bonds. A strong Brönsted acid sites in pyridine sulfonic acid may form H-bonding between the Hydroxyl groups of pyridine sulfonic acid with of the oxygen of β-glycosidic bonds [1-4]. A cyclic carbonium ion could be formed as a result of C–O bond cleavage which yield monosaccharides after partial hydrolyses Scheme 3.4.

However, the glucose formed was also degraded over the pyridine sulfonic acid to give CO_2 as determined by GC-MAS.

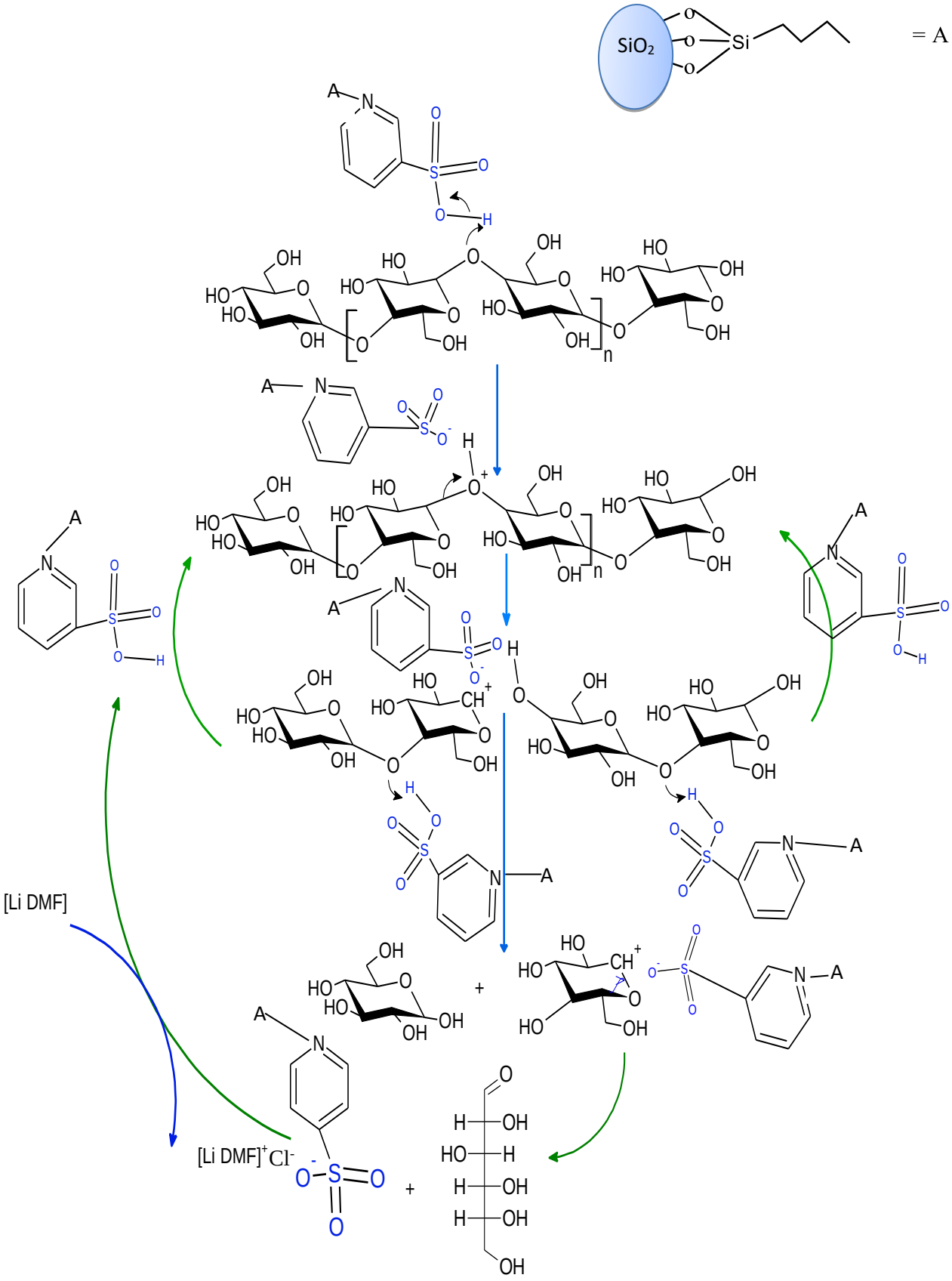

Scheme 3.4: The suggested mechanism of cellulose hydrolysis over heterogeneous catalyst.

Chapter Four

Conclusions and Recommendation

4.0 Conclusions and Recommendation

4.1 Conclusions

In comparing the direct and reflux methods for both catalyst RHAPSA@Dir and RHAPSA@Ref, it was found that the catalyst prepared by the direct method is more effective in the hydrolysis of cellulose and the degradation of glucose into other products. Both the Si – O -Si ,SO_2 , and band and the CH aromatic and aliphatic were detectable by FT-IR, as expected. According to the data collected by BET RHAPSA@Dir, catalyst had 416 m^2 g^{-1} as specific surface area and RHAPSA@Ref had 50 m^2 g^{-1}. Catalyst stability at a temperature of 250 ^oC has been demonstrated using thermogravimetric analysis (TGA). The catalyst structures of RHAPSA@Dir and RHAPSA@Ref, as determined by CHNS analysis, showed the presence both sulfur and nitrogen.

Hydrolysis conditions were optimized by investigating the effects of mass, temperature, solvents, and other parameters on the final product. Results showed that 0.1 gm was the best mass used for cellulose hydrolysis, and 0.15 gm was the best mass for glucose degradation. All masses were run at 140 °C for 10 hours in glucose degradation and 13 hours in cellulose experiments. DMF showed that cellulose hydrolysis can easily while 1-Butanol glucose degradation can easily.

RHAPSA@Dir needed 9 h to hydrolyze 55 % of cellulose and 4 h to hydrolyze 86% of glucose.RHAPSA@Ref needed 10 h to hydrolyze 41% of cellulose and 4 h to hydrolyze 80% of glucose. As a results of any amount of glucose are directly degraded into other products, especially in the first six hours, and this shows the high effectiveness of the catalyst on glucose degradation more than the hydrolysis of

cellulose into glucose. The catalyst has been reused several times and has proven effective for cellulose and glucose hydrolysis.

4.2 Recommendations

1-The suggested mechanism needs more study.

2-Charactrazation of used catalyst and it's compared with the first one.

3-The kinetic study is very imported to catalyst the activation energy and reaction order.

References

References

[1] Z. Yu, X. Lu, J. Xiong, and N. Ji, "Transformation of Levulinic Acid to Valeric Biofuels: A Review on Heterogeneous Bifunctional Catalytic Systems," *Chemistry-sustainability-Energy-Materials*,vol.12,no. 17, pp. 3915–3930,2019, doi: 10.1002/CSSC.201901522.

[2] Z. Yu, X. Lu, C. Liu, Y. Han, and N. Ji, "Synthesis of γ-valerolactone from different biomass-derived feedstocks: Recent advances on reaction mechanisms and catalytic systems," *Renewable and Sustainable Energy Reviews*, vol. 112, pp. 140–157, 2019, doi: 10.1016/J.RSER.2019.05.039.

[3] S. Kim and B. E. Dale, "Global potential bioethanol production from wasted crops and crop residues," *Biomass Bioenergy*, vol. 26, no. 4, pp. 361–375, 2004, doi: 10.1016/J.BIOMBIOE.2003.08.002.

[4] X. Li Xiaoyun Li, Xuebin Lu, Min Liang, Rui Xu , Zhihao Yu , Bingyu Duan , Lefu Lu., "Conversion of waste lignocellulose to furfural using sulfonated carbon microspheres as catalyst," *Waste Management*, vol. 108, pp. 119–126, 2020, doi: 10.1016/J.WASMAN.2020.04.039.

[5] R. S. Dhillon and G. von Wuehlisch, "Mitigation of global warming through renewablebiomass,"*BiomassBioenergy*,vol.48,pp.75–89,2013,doi: 10.1016/J.BIOMBIOE.2012.11.005.

[6] D. Klemm Dieter K, Emily D. Cranston, Dagmar F, Miguel G, Stephanie A. Kedzior , Dana K, Friederike k, Tetsuo K, Tom L, Sandor N, Katrin P, Falk R., "Nanocellulose as a natural source for groundbreaking applications in materials science: Today's state," *Materials Today*, vol. 21, no. 7, pp. 720–748, 2018, doi: 10.1016/J.MATTOD.2018.02.001.

[7] Q. Wang, Q. Yao, J. Liu, J. Sun, Q. Zhu, and H. Chen, "Processing nanocellulose to bulk materials: a review," *Cellulose 2019 26:13*, vol. 26, no. 13, pp. 7585–7617, 2019, doi: 10.1007/S10570-019-02642-3.

[8] D. Trache Klemm D, Cranston ED, Fischer D, Gama M, Kedzior SA, Kralisch D., "Nanocellulose: From Fundamentals to Advanced Applications, *Frontiers inChemistry*,vol. 8, p. 392, 2020, doi: 10.3389/FCHEM.2020.00392/BIBTEX.

[9] T. Wang, M. W. Nolte, and B. H. Shanks, "Catalytic dehydration of C6 carbohydrates for the production of hydroxymethylfurfural (HMF) as a versatile platform chemical," *Green Chemistry*, vol. 16, no. 2, pp. 548–572, 2014, doi: 10.1039/C3GC41365A.

[10] B. Saha and M. M. Abu-Omar, "Advances in 5-hydroxymethylfurfural production from biomass in biphasic solvents," *Green Chemistry*, vol. 16, no. 1, pp. 24–38, 2013, doi: 10.1039/C3GC41324A.

[11] M. Morales, J. Quintero, R. Conejeros, and G. Aroca, "Life cycle assessment of lignocellulosic bioethanol: Environmental impacts and energy balance," *Renewable and Sustainable Energy Reviews*, vol. 42, pp. 1349–1361, 2015, doi: 10.1016/J.RSER.2014.10.097.

[12] Z. Yu, X. Lu, H. Bai, J. Xiong, W. Feng, and N. Ji, "Effects of Solid Acid Supports on the Bifunctional Catalysis of Levulinic Acid to γ-Valerolactone: Catalytic Activity and Stability," *Chemistry—An Asian*, vol. 15, no. 8, pp. 1182–1201, 2020, doi: 10.1002/ASIA.202000006.

[13] X. Zheng, X. Gu, Y. Ren, Z. Zhi, and X. Lu, "Production of 5-hydroxymethyl furfural and levulinic acid from lignocellulose in aqueous solution and different solvents," *Biofuels, Bioproducts and Biorefining*, vol. 10, no. 6, pp. 917–931, 2016, doi: 10.1002/BBB.1720.

[14] J. J. Bozell and G. R. Petersen, "Technology development for the production of biobased products from biorefinery carbohydrates—the US Department of Energy's 'Top 10' revisited," *Green Chemistry*, vol. 12, no. 4, pp. 539–554, 2010, doi: 10.1039/B922014C.

[15] T. D. Hoang and N. Nghiem, "Recent Developments and Current Status of Commercial Production of Fuel Ethanol," *Fermentation 2021, Vol. 7, Page 314*, vol. 7, no. 4, p. 314, 2021, doi: 10.3390/FERMENTATION7040314.

[16] "Biofuels explained - data and statistics - U.S. Energy Information Administration(EIA)."Accessed:23,2023..Available: https://www.eia.gov/energyexplained/biofuels/data-and-statistics.php

[17] S. Kim and B. E. Dale, "Global potential bioethanol production from wasted crops and crop residues," *Biomass Bioenergy*, vol. 26, no. 4, pp. 361–375, 2004, doi: 10.1016/J.BIOMBIOE.2003.08.002.

[18] P. McKendry, "Energy production from biomass (part 1): overview of biomass," *Bioresource Technology*, vol. 83, no. 1, pp. 37–46, 2002, doi: 10.1016/S0960-8524(01)00118-3.

[19] W. A, G. M, R. C, R. A, and Z. G, "Effect of reduction in yeast and enzyme concentrations in a simultaneous- saccharification-and-fermentation-based bioethanol process: technical and economic evaluation," *Applied Biochemistry and Biotechnology*, vol. 121–124, 2005, doi: 10.1385/ABAB:122:1-3:0485.

[20] Y. Yue, "LSU Digital Commons Cellulose Nanofibers from Energycane Bagasse and Their Applications in Core-Shell Structured Hydrogels cellulose nanofibers from energycane bagasse and their applications in core-shell structured hydrogels The School of Renewable Natural Resources", Accessed: 12,2023.

[21] T. Nishino, I. Matsuda, and K. Hirao, "All-Cellulose Composite," *Macromolecules*, vol. 37, no. 20, pp. 7683–7687, 2004, doi: 10.1021/MA049300H.

[22] K. M. Hello, H. H. Mihsen, M. J. Mosa, and M. S. Magtoof, "Hydrolysis of cellulose over silica-salicylaldehyde phenylhydrazone catalyst," *Taiwan Institute of Chemical Engineers*, vol. 46, pp. 74–81, 2015, doi: 10.1016/J.JTICE.2014.09.005.

[23] S. Roy, S. Panja, S. R. Sahoo, S. Chatterjee, and D. Maiti, "Enroute sustainability: metal free C–H bond functionalisation," *Chemical Society Reviews*, 2023, doi: 10.1039/D0CS01466D.

[24] F. Delbecq, Y. Wang, A. Muralidhara, K. E. El Ouardi, G. Marlair, and C. Len, "Hydrolysis of hemicellulose and derivatives-a review of recent advances in the production of furfural," *Frontiers in Chemistry*, vol. 6, no. MAY, 2018, doi: 10.3389/FCHEM.2018.00146.

[25] B. Waliszewska, M. Mleczek, M. Zborowska, P. Goliński, P. Rutkowski, and K. Szentner, "Changes in the chemical composition and the structure of cellulose and lignin in elm wood exposed to various forms of arsenic," *Cellulose*, vol. 26, no. 10, pp. 6303–6315, 2019, doi: 10.1007/S10570-019-02511-Z/FIGURES/2.

[26] A. Arora, P. Nandal, J. Singh, and M. L. Verma, "Nanobiotechnological advancements in lignocellulosic biomass pretreatment," *Materials Science for EnergyTechnologies*,vol.3,pp.308–318,2020,doi: 10.1016/J.MSET.2019.12.003.

[27] L. Donaldson, "Cellulose microfibril aggregates and their size variation with cell wall type," *Wood Science and Technol*ogy, vol. 41, no. 5, pp. 443–460, 2007, doi: 10.1007/S00226-006-0121-6/METRICS.

[28] M. Ashaduzzaman and S. Shamsuddin, "Studies on Interaction of Lidocaine Drug with Natural Cellulosic Fibres Article in," *International Journal of Pharmacology Phytochemistry and Ethnomedicine*, 2016, doi: 10.18052/www.scipress.com/IJPPE.4.36.

[29] J. Bengtsson, "Thesis for the degree of licentiate of engineering Spinning of lignin-cellulose carbon-fiber precursors". 2019. Chalmers University of Technology. PhD thesis.

[30] S Elisabeth, G Kristina, P Bert, C Anders "Characterization of the cellulosic residues from lithium chloride/N,N-dimethylacetamide dissolution of softwood kraft pulp," *Carbohydrate Polymers*, vol. 32, no. 1, pp. 57–63, 1997, doi: 10.1016/S0144-8617(96)00129-4.

[31] K. M. Hello, H. R. Hasan, M. H. Sauodi, and P. Morgen, "Cellulose hydrolysis over silica modified with chlorosulphonic acid in one pot synthesis," *Applied Catalysis A General*, vol. 475, pp. 226–234, 2014, doi: 10.1016/J.APCATA.2014.01.035.

[32] Y. B. Huang and Y. Fu, "Hydrolysis of cellulose to glucose by solid acid catalysts," *Green Chemistry*, vol. 15, no. 5, pp. 1095–1111, 2013, doi: 10.1039/C3GC40136G.

[33] D. M. Lai, L. Deng, J. Li, B. Liao, Q. X. Guo, and Y. Fu, "Hydrolysis of Cellulose into Glucose by Magnetic Solid Acid," *ChemistrySustainability-Energy- Materials*, vol. 4, no. 1, pp. 55–58, 2011, doi: 10.1002/CSSC.201000300.

[34] M. Muhaimin, B. Wiyantoko, R. N. Putri, and R. Rusitasari, "Determination of order reaction on hydrolysis reaction of pineapple leaf," AIP Confernce Proceedings, vol. 2026,2018, doi: 10.1063/1.5065010.

[35] N. F. Vasconcelos Vasconcelos N, Feitosa J, da Gama F, Morais J, Andrade F, de Souza Filho M, Rosa M., "Bacterial cellulose nanocrystals produced under different hydrolysis conditions: Properties and morphological features," *Carbohydr Polym*, vol. 155, pp. 425–431, 2017, doi: 10.1016/J.CARBPOL.2016.08.090.

[36] A. Onda, T. Ochi, and K. Yanagisawa, "Selective hydrolysis of cellulose into glucose over solid acid catalysts," *Green Chemistry*, vol. 10, no. 10, pp. 1033–1037, 2008, doi: 10.1039/B808471H.

[37] J. S. Kim, Y. Y. Lee, and R. W. Torget, "Cellulose hydrolysis under extremely low sulfuric acid and high-temperature conditions," *Applied Biochemistry and Biotechnology - Part A Enzyme Engineering and Biotechnology*, vol. 91–93, no. 1, pp. 331–340, 2001, doi: 10.1385/ABAB:91-93:1-9:331/METRICS.

[38] E. M. Sulman Sulman E, Matveeva V, Manaenkov O, Filatova A, Kislitza O, Doluda V, Rebrov E, Sidorov A, Shimanskaya E., "Cellulose hydrogenolysis with the use of the catalysts supported on hypercrosslinked polystyrene," *AIP Conf Proc*, vol. 1787, no. 1, p. 030004, Nov. 2016, doi: 10.1063/1.4968069.

[39] S. Suganuma, K Nakajima, M Kitano, D Yamaguchi, H Kato, S Hayashi, M Hara *l.*, "Hydrolysis of cellulose by amorphous carbon bearing SO3H, COOH, and OH groups," *Journalof theAmerican Chemical Soc*iety, vol. 130, no. 38, pp. 12787–12793,2008,doi: 10.1021/JA803983H/SUPPL_FILE/JA803983H_SI_001.PDF.

[40] B. Wiredu and A. S. Amarasekara, "Synthesis of a silica-immobilized Brönsted acidic ionic liquid catalyst and hydrolysis of cellulose in water under

mild conditions," *Catalysis Commun*ications, vol. 48, pp. 41–44, 2014, doi: 10.1016/J.CATCOM.2014.01.021.

[41] H. Kobayashi, H. Ohta, and A. Fukuoka, "Conversion of lignocellulose into renewable chemicals by heterogeneous catalysis," *Catalysis Science and Technol*ogy, vol. 2, no. 5, pp. 869–883, 2012, doi: 10.1039/C2CY00500J.

[42] A. Takagaki, M. Nishimura, S. Nishimura, and K. Ebitani, "Hydrolysis of Sugars Using Magnetic Silica Nanoparticles with Sulfonic Acid Groups," 2011, doi: 10.1246/cl.2011.1195.

[43] G. Fan, C. Liao, T. Fang, M. Wang, and G. Song, "Hydrolysis of cellulose catalyzed by sulfonated poly(styrene-co-divinylbenzene) in the ionic liquid 1-n-butyl-3-methylimidazolium bromide," *Fuel Processing Technology*, vol. 116, pp. 142–148, 2013, doi: 10.1016/J.FUPROC.2013.05.009.

[44] Y. H. Percival Zhang, J. Cui, L. R. Lynd, and L. R. Kuang, "A transition from cellulose swelling to cellulose dissolution by o-phosphoric acid: Evidence from enzymatic hydrolysis and supramolecular structure," *Biomacromolecules*,vol.7,no.2,pp.644–648,2006,doi: 10.1021/BM050799C/ASSET/IMAGES/BM050799C.SOCIAL.JPEG_V03.

[45] F. Chambon, F. Rataboul, C. Pinel, A. Cabiac, E. Guillon, and N. Essayem, "Cellulose hydrothermal conversion promoted by heterogeneous Brønsted and Lewis acids: Remarkable efficiency of solid Lewis acids to produce lactic acid," *Applied Catalysis B*, vol. 105, no. 1–2, pp. 171–181, 2011, doi: 10.1016/J.APCATB.2011.04.009.

[46] L. Shuai and X. Pan, "Hydrolysis of cellulose by cellulase-mimetic solid catalyst," *Energy and Environmental Sci*ence, vol. 5, no. 5, pp. 6889–6894,. 2012, doi: 10.1039/C2EE03373A.

[47] A. S. Amarasekara and B. Wiredu, "A comparison of dilute aqueous p-toluenesulfonic and sulfuric acid pretreatments and saccharification of corn stover at moderate temperatures and pressures," *Bioresour Technol*, vol. 125, pp. 114–118, 2012, doi: 10.1016/J.BIORTECH.2012.08.112.

[48] H. Cai, C. Li, A. Wang, G. Xu, and T. Zhang, "Zeolite-promoted hydrolysis of cellulose in ionic liquid, insight into the mutual behavior of zeolite, cellulose and ionic liquid," *Applied Catalysis B*, vol. 123–124, pp. 333–338, 2012, doi: 10.1016/J.APCATB.2012.04.041.

[49] H. Wang, C. Zhang, H. He, and L. Wang, "Glucose production from hydrolysis of cellulose over a novel silica catalyst under hydrothermal conditions," *Journal of Environmental Sciences*, vol. 24, no. 3, pp. 473–478, 2012, doi: 10.1016/S1001-0742(11)60795-X.

[50] D. Verma, R. Tiwari, and A. K. Sinha, "Depolymerization of cellulosic feedstocks using magnetically separable functionalized graphene oxide," *Royal Society of chemistry* , vol. 3, no. 32, pp. 13265–13272, 2013, doi: 10.1039/C3RA41025K.

[51] B. Velaga and N. R. Peela, "Levulinic acid production from furfural: process development and techno-economics," *Green Chemistry*, vol. 24, no. 8, pp. 3326–3343, 2022, doi: 10.1039/D2GC00089J.

[52] G. Leofanti, G. Tozzola, M. Padovan, G. Petrini, S. Bordiga, and A. Zecchina, "Catalyst characterization: characterization techniques," *Catalyst Today*, vol. 34, no. 3–4, pp. 307–327, 1997, doi: 10.1016/S0920-5861(96)00056-9.

[53] J. Hagen, "Industrial Catalysis: A Practical Approach: Second Edition," *Industrial Catalysis: A Practical Approach: Second Edition*, pp. 1–507, 2006, doi: 10.1002/3527607684.

[54] M. E. Davis and R. J. Davis, Fundamentals of chemical reaction engineering. *Technology & Engineering*, McGraw-Hill, 2003.

[55] E. Farnetti, R. Monte, and J. Kašpar, "Homogeneous and heterogeneous catalysis," Inorg. and Bio-inorg. Chem. (2006). 2, 1-10.

[56] J. Kamau, A. Ahmed, F. Hyndman, P. Hirst, and J. Kangwa, "Influence of Rice Husk Ash Density on the Workability and Strength of Structural Concrete," *European Journal of Engineering Research and Science*, vol. 2, no. 3, p. 36, 2017, doi: 10.24018/EJERS.2017.2.3.292.

[57] S. K. S. Hossain, L. Mathur, and P. K. Roy, "Rice husk/rice husk ash as an alternative source of silica in ceramics: A review," *https://doi.org/10.1080/21870764.2018.1539210*, vol. 6, no. 4, pp. 299–313, 2018, doi: 10.1080/21870764.2018.1539210.

[58] C. N. Djangang, S. Mlowe, D. Njopwouo, and N. Revaprasadu, "One-step synthesis of silica nanoparticles by thermolysis of rice husk ash using non toxic chemicals ethanol and polyethylene glycol.," *Journal of Applicable Chemistry*, vol. 4, no. 4, pp. 1218–1226, 2015.

[59] R. Prasad and M. Pandey, "Rice Husk Ash as a Renewable Source for the Production of Value Added Silica Gel and its Application: An Overview," *Bulletin of Chemical Reaction Engineering & Catalysis*, vol. 7, no. 1, pp. 1–25, 2012.

[60] R. Pode, "Potential applications of rice husk ash waste from rice husk biomass power plant," *Renewable and Sustainable Energy Reviews*, vol. 53, pp. 1468–1485, 2016, doi: 10.1016/J.RSER.2015.09.051.

[61] J. A. Santana Costa and C. M. Paranhos, "Systematic evaluation of amorphous silica production from rice husk ashes," *Journal Cleaner Prod*uction, vol. 192, pp. 688–697, 2018, doi: 10.1016/J.JCLEPRO.2018.05.028.

[62] M. A. Tambichik, N. Mohamad, A. A. A. Samad, M. Z. M. Bosro, and M. A. Iman, "Utilization of construction and agricultural waste in Malaysia for development of Green Concrete: A Review," in *IOP Conference Series: Earth and Environmental Science*, Institute of Physics Publishing, 2018. doi: 10.1088/1755-1315/140/1/012134.

[63] J. Wang and X. Guo, "Adsorption kinetic models: Physical meanings, applications, and solving methods," *Journal of Hazardous Mater*ials, vol. 390, p. 122156, 2020, doi: 10.1016/J.JHAZMAT.2020.122156.

[64] Y. Shen, "Rice husk silica derived nanomaterials for sustainable applications," *Renewable and Sustainable Energy Reviews*, vol. 80, pp. 453–466, Dec. 2017, doi: 10.1016/J.RSER.2017.05.115.

[65] N. K. Sharma, W. S. Williams, and A. Zangvil, "Formation and Structure of Silicon Carbide Whiskers from Rice Hulls," *Journal of the American Ceramic Society*, vol. 67, no. 11, pp. 715–720, 1984, doi: 10.1111/J.1151-2916.1984.TB19507.X.

[66] Y. Shen, "Rice husk silica derived nanomaterials for sustainable applications," *Renewable and Sustainable Energy Reviews*, vol. 80, pp. 453–466, 2017, doi: 10.1016/J.RSER.2017.05.115.

[67] H. H. Mihsen, D. Hussien "Synthesis and Characterization of Organosilicon Ligands and Used it in Removal of Some Divalent Metal Ions from their Aqueous Solutions project", Accessed: 24, 2023.. Available: https://www.researchgate.net/publication/332290653

[68] P. K. Jal, S. Patel, and B. K. Mishra, "Chemical modification of silica surface by immobilization of functional groups for extractive concentration of metal ions," *Talanta*, vol. 62, no. 5, pp. 1005–1028, 2004, doi: 10.1016/j.talanta.2003.10.028.

[69] C. Xiao, P. Shi, W. Yan, L. Chen, L. Qian, and S. H. Kim, "Thickness and structure of adsorbed water layer and effects on adhesion and friction at nanoasperity contact," *Colloids and Interfaces*, vol. 3, no. 3. MDPI AG, 2019. doi: 10.3390/colloids3030055.

[70] C. Pavan Pavan C, Delle Piane M, Gullo M, Filippi F, Fubini B, Hoet P, Horwell C, Huaux F, Lison D, Lo Giudice C, Martra G., "The puzzling issue of silica toxicity: Are silanols bridging the gaps between surface states and pathogenicity?" *Particle Fibre Toxicol*ogy, vol. 16, no. 1, pp. 1–10, 2019, doi: 10.1186/S12989-019-0315-3/FIGURES/1.

[71] H. Salman Sobh Al-Tai and A. Hayder Hamied Al-Hmedawi, "Synthesis and Characterization of Organosilicon Catalyst for Cellulose Hydrolysis Supervision by Msc thesis University of Kerbala" 2017.

[72] D. A. Stenger Stenger D, Dulcey C, Rudolph A, Calvert J, George J, Georger J, Hickman J, Nielsen T, McCort S, McCort S., "Coplanar Molecular Assemblies of Amino- and Perfluorinated Alkyl silanes: Characterization and Geometric Definition of Mammalian Cell Adhesion and Growth," *J Am Chem Soc*,vol.114,no.22,pp.8435–8442,1992,doi: 10.1021/JA00048A013/ASSET/JA00048A013.FP.PNG_V03.

[73] V. A. Tertykh and L. A. Belyakova, "Chapter 1.6 Solid-phase hydrolyzation reactions with participation of modified silica surface," *Studies in Surface Science Catal*ysis, vol. 99, pp. 147–189,1996, doi: 10.1016/S0167-2991(06)81020-7.

[74] S. Dash, S. Mishra, S. Patel, and B. K. Mishra, "Organically modified silica: Synthesis and applications due to its surface interaction with organic molecules," *Advances Colloid Interface Sci*ence, vol. 140, no. 2, pp. 77–94, 2008, doi: 10.1016/J.CIS.2007.12.006.

[75] L. Peng, W. Qisui, L. Xi, and Z. Chaocan, "Investigation of the states of water and OH groups on the surface of silica," *Colloids and Surface A Physicochem Eng*vol.334,no.1–3,pp.112–115,Feb.2009,doi: 10.1016/J.COLSURFA.2008.10.028.

[76] A. R. Cestari, E. F. S. Vieira, R. E. Bruns, and C. Airoldi, "Some New Data for Metal Desorption on Inorganic–Organic Hybrid Materials," *Journal of Colloid andInterfaceSci*ence,vol.227,no.1,pp.66–70,2000,doi: 10.1006/JCIS.2000.6841.

[77] D. Hoegaerts, B. F. Sels, D. E. de Vos, F. Verpoort, and P. A. Jacobs, "Heterogeneous tungsten-based catalysts for the epoxidation of bulky olefins," *Catalyst Today*, vol. 60, no. 3–4, pp. 209–218,2000, doi: 10.1016/S0920-5861(00)00337-0.

[78] A. G. S. Prado and C. Airoldi, "The Pesticide 3-(3,4-Dichlorophenyl)-1,1-dimethylurea (Diuron) Immobilized on Silica Gel Surface," *Journal Colloid Interface Sci*ence, vol. 236, no. 1, pp. 161–165, 2001, doi: 10.1006/JCIS.2000.7401.

[79] F. Habeche Habeche F, Hachemaoui M, Mokhtar A, Chikh K, Benali F, Mekki A, Zaoui F, Cherifi Z, Boukoussa B., "Recent Advances on the Preparation and Catalytic Applications of Metal Complexes Supported-Mesoporous Silica MCM-41 (Review)," *Journal Inorg Organomet Polym Mater*, vol. 30, no. 11, pp. 4245–4268, 2020, doi: 10.1007/S10904-020-01689-1/METRICS.

[80] F. Adam, K. M. Hello, and H. Osman, "Synthesis of Mesoporous Silica Immobilized with 3-[(Mercapto or amino)propyl]trialkoxysilane by a Simple One-pot Reaction," *Chinese Journal of Chemistry*, vol. 28, no. 12, pp. 2383–2388, 2010, doi: 10.1002/CJOC.201190008.

[81] F. Adam, K. M. Hello, and S. J. Chai, "The heterogenization of l-phenylalanine–Ru(III) complex and its application as catalyst in esterification of ethyl alcohol with acetic acid," *Chemical Engineering Research and Design*,vol.90 no. 5, pp. 633–642, 2012, doi: 10.1016/J.CHERD.2011.09.009.

[82] M. Laspéras, T. Llorett, L. Chaves, I. Rodriguez, A. Cauvel, and D. Brunel, "Amine functions linked to MCM-41-type silicas as a new class of solid base catalysts for condensation reactions," *Studies in Surface Science and Catal*ysis, vol. 108, pp. 75–82, J1997, doi: 10.1016/S0167-2991(97)80890-7.

[83] K. Mohammed, "the heterogenation of saccharin, melamine and sulfonic acid onto rice husk ash silica and their catalytic activity in esterification reaction Hydrolysis of cellulose by simple methods View project Simplest method for preparing any heterogeneous catalyst View project," 2010, doi: 10.13140/RG.2.2.29743.94882.

[84] F. Adam, H. E. Hassan, and K. M. Hello, "The synthesis of N-heterocyclic carbene–silica nano-particles and its catalytic activity in the cyclization of glycerol," *Journal of thaiwan Institute of Chemical Engineers*, vol. 43, no. 4, pp. 619–630, 2012, doi: 10.1016/J.JTICE.2012.01.013.

[85] R. Gupta, S. Paul, and R. Gupta, "Covalently anchored sulfonic acid onto silica as an efficient and recoverable interphase catalyst for the synthesis of 3,4-dihydropyrimidinones/thiones," *Journal of ofMolecular Catalysis A*, vol. 266, no. 1–2, pp. 50–54, 2007, doi: 10.1016/J.MOLCATA.2006.10.039.

[86] W. D. Bossaert, D. E. de Vos, W. M. van Rhijn, J. Bullen, P. J. Grobet, and P. A. Jacobs, "Mesoporous Sulfonic Acids as Selective Heterogeneous Catalysts for the Synthesis of Monoglycerides," *Journal Catal*ysis, vol. 182, no. 1, pp. 156–164, 1999, doi: 10.1006/JCAT.1998.2353.

[87] M. J. Climent, A. Velty, and A. Corma, "Design of a solid catalyst for the synthesis of a molecule with blossom orange scent," *Green Chemistry*, vol. 4, no. 6, pp. 565–569, 2002, doi: 10.1039/B207506G.

[88] F. Adam, K. M. Hello, and T. H. Ali, "Solvent free liquid-phase alkylation of phenol over solid sulfanilic acid catalyst," *Applied Catalysis A Gen*, vol. 399, no. 1–2, pp. 42–49, 2011, doi: 10.1016/J.APCATA.2011.03.039.

[89] T. J. Al-Hasani, H. H. Mihsen, K. M. Hello, and F. Adam, "Catalytic esterification via silica immobilized p-phenylenediamine and dithiooxamide

solid catalysts," *Arabian Journal of Chemistry*, vol. 10, pp. S1492–S1500, 2017, doi: 10.1016/j.arabjc.2013.04.030.

[90] K. M. Hello, A. K. T. Mohammad, and A. G. Sager, "Solid Urea Sulfate Catalyst for Hydrolysis of Cellulose," *Waste Biomass Valorization*, vol. 8, no. 8, pp. 2621–2630, 2017, doi: 10.1007/S12649-016-9693-Z/METRICS.

[91] A. E. Ahmed and F. Adam, "Indium incorporated silica from rice husk and its catalytic activity," *Microporous and Mesoporous Materials*, vol. 103, no. 1–3, pp. 284–295, 2007, doi: 10.1016/J.MICROMESO.2007.01.055.

[92] F. Adam, H. Osman, and K. M. Hello, "The immobilization of 3-(chloropropyl)triethoxysilane onto silica by a simple one-pot synthesis," *Journal of Colloid and Interface Sci*ence, vol. 331, no. 1, pp. 143–147, 2009, doi: 10.1016/J.JCIS.2008.11.048.

[93] G. L. Miller, "Use of Dinitrosalicylic Acid Reagent for Determination of Reducing Sugar," *Analytical Chemistry*, vol. 31, no. 3, pp. 426–428, 1959, doi: 10.1021/AC60147A030/ASSET/AC60147A030.FP.PNG_V03.

[94] J. B. Sumner and V. A. Graham, "dinitrosalicylic acid: a reagent for the estimation of sugar in normal and diabetic urine," *Journal of Biological Chemistry*, vol. 47, no. 1, pp. 5–9, 1921, doi: 10.1016/S0021-9258(18)86093-8.

[95] Y. Bai Bai Y, Liu H, Ma X, Tai X, Wang W, Du Z, Wang G., "Synthesis, characterization and physicochemical properties of glycosyl-modified polysiloxane," *Journal of Molecular Liq*uids, vol. 266, pp. 90–98,2018, doi: 10.1016/J.MOLLIQ.2018.06.052.

[96] P. O. Yablonsky, A. V. Tarasov, Y. A. Moskvichev, and O. P. Yablonsky, "Research of a structure and association of saccharine derivatives," *Journal of Molecular Liq*uids, vol. 91, no. 1–3, pp. 223–229, 2001, doi: 10.1016/S0167-7322(01)00166-0.

[97] I. Díaz, F. Mohino, J. Pérez-Pariente, and E. Sastre, "Synthesis, characterization and catalytic activity of MCM-41-type mesoporous silicas functionalized with sulfonic acid," *Applied Catalysis A Gen*eral, vol. 205, no. 1–2, pp. 19–30, 2001, doi: 10.1016/S0926-860X(00)00808-5.

[98] L. T. Zhuravlev, "The surface chemistry of amorphous silica. Zhuravlev model," *Colloids and Surfaces A Physicochemical Engineering* vol. 173, no. 1–3, pp. 1–38, Nov. 2000, doi: 10.1016/S0927-7757(00)00556-2.

[99] A. K. Ladavos, A. P. Katsoulidis, A. Iosifidis, K. S. Triantafyllidis, T. J. Pinnavaia, and P. J. Pomonis, "The BET equation, the inflection points of N2 adsorption isotherms and the estimation of specific surface area of porous

solids," *Microporous and Mesoporous Materials*, vol. 151, pp. 126–133, 2012, doi: 10.1016/J.MICROMESO.2011.11.005.

[100] W. Marsden, P. P. Gray, G. J. Nippard, and M. R. Quinlan, "Evaluation of the DNS method for analysing lignocellulosic hydrolysates," *Journal of Chemical Technology and Biotechnology*, vol. 32, no. 7–12, pp. 1016–1022, 1982, doi: 10.1002/JCTB.5030320744.

الخلاصة

في هذه الدراسة تم استخلاص السليكا من قشور الرز عن طريق غسل قشور الرز مرات عديدة بالماء المقطر، ثم عوملت مع محلول (1.0M) من حامض النتريك، بعد ذلك حرقت في فرن بدرجة حرارة 800 درجة مئوية ، تم تحويل السليكا الناتجة إلى سيليكات الصوديوم بعد اذابتها بمحلول (1.0M) من هيدروكسيد الصوديوم ثم بعد ذلك تم مفاعلتها مع 3-(كلورو بروبيل) ثلاثي ايثوكسي سيلاين CPTES ينتج سليكا ذات مجموعة وظيفية $-CH_2-Cl$ رمز لها بالرمز RHACCl .

تحميل بريدين حامض السلفونيك على سطح السليكا بطريقتين طريق الخطوة الواحدة تم اضافة بريدين حامض السلفونيك وCPTES وسليكات الصوديوم في المحلول المائي ثم تسحيح الخليط ضد HNO_3 (3.0N) و طريقة التصعيد الارجاعي حيث تم اضافة RHACCl وبريدين حامض السلفونيك الى مذيب التلوين وبدرجة حرارة 120 درجة مئوية لمدة 48 ساعة تكون العامل المساعد الغير المتجانس رمز له RHAPSA@Dir RHAPSA@Ref, على التوالي .

تشخيص العامل المساعد المحضر بعدة تقنيات منها تحليل العناصر (CHNS) حيث ظهور نسب النتروجين والكبريت. التحلل الحراري TGA/DSC حيث اثبت الاستقرار الحراري لكلا المحفزين حتى درجة 250 درجة مئوية وطبقا لتحليل امتزاز النيتروجين وجدت المساحة السطحيه للعامل المساعد الغير متجانس 50 416 m^2/gm, لكلا الطريقتين الخطوة الواحدة والتصعيد الارجاعي على التوالي. اظهرت مطيافية الأشعة تحت الحمراء FT-IR حيث ظهور حزمة لل SO_2 وCH الحلقة الارماتية لم يظهر فحص FT-IR اي تغير بالمجاميع الوظيفية للعامل المساعد المحظر في كلا الطريقتين. المجهر الالكتروني الماسح SEM والمجهر الالكتروني النافذ TEM الذي بين تظاريس وحجم وترتيب الجسيمات للعامل المساعد . اظهرت نتائج حيود الاشعة السينية لكلا العاملين المساعدين ضهور حزمة عريضة عند زاوية 22^o والذي يثبت ان السطح غير بلوري.

تحلل السليلوز و الكلوكوز على سطح العامل المساعد غير المتجانس وكذلك المتجانس.احتاج العامل المساعد المتجانس 3الى 6 ساعات لتحلل السليلوز يعطي نسبة تحلل 98% وتحلل الكلوكوز بنسبة 92% وهذا يعود الى طبيعة العامل المساعد طبيعة فيزيائية التي تجعله بتماس مع جزيئات المادة المحلله. اما العامل المساعد غير المتجانس المحضر بالطريقة الخطوة الواحدة احتاج الى 9 ساعات ليتحلل السليلوز بنسبة 55% وفي التجربة

الاخرى لتحلل الكلوكوز احتاج الى 4 ساعات ليعطي نسبة تحلل 86% هذ يدل على ان العامل المساعد تأثيرة اكبر على تحلل الكلوكوز الى منتجات اخرى وهذا يبين عدم وجود كميات تراكمية من الكلوكوز المتحلل من السليلوز أي ان أي كمية تتحلل من السليلوز يتم تحللها مباشرتا الى منتجات اخرى . اما العامل المحضر بطريقة التصعيد الارجاعي احتاج الى 10 ساعات ليتحلل السليلوز بنسبة 41% وفي التجربة الاخرى لتحلل الكلوكوز احتاج الى 4 ساعات ليتحلل بنسبة 80% .لذلك الفعالية التحفيزية للعوامل المساعدة التي استخدمت في تحلل السليلوز وتحلل الكلوكوز الى مركبات اخرى يمكن ان تتبع التسلسل الاتي :

Pyridine sulfonic acid > RHAPSA@Dir > RHAPSA@Ref

جمهورية العراق

وزارة التعليم العالي والبحث العلمي

جامعة المثنى/ كلية العلوم

قسم الكيمياء

تحلل السليلوز والكلوكوز على سطح السليكا- بريدين سلفونك أسد

رسالة مقدمة الى

مجلس كلية العلوم /جامعة المثنى

وهي جزء من متطلبات نيل درجة الماجستير في علوم الكيمياء

من قبل

حسين عبدالباري زويد

بكالوريوس علوم كيمياء 2009

بأشراف

أ. د. قاسم محمد حلو

1444هـ **2023 م**